AN ANALYSER FOR VELOCITY MODULATED ELECTRON BEAMS

by

R.A. McFarlane

A thesis submitted to the Faculty of Graduate Studies and Research at McGill University in partial fulfilment of the requirements for the degree of Master of Science.

The Eaton Electronics Research Laboratory,

McGill University, Montreal.

April, 1955.

TABLE OF CONTENTS

ABSTRACT

An analyser for the examination of velocity modulated electron beams has been designed and built. The analysis was achieved by displaying on a fluorescent screen the density and velocity variations in the electron stream at a particular point along the beam. Two sets of Lecher wires were placed at right angles and driven from the same signal source as was used to modulate the beam. The electron beam passed between each set of wires and by properly phasing the voltages across the wires, a circular trace was obtained on the screen placed to intercept the beam. Density and velocity variations in the beam appeared as changes in trace intensity and radial position respectively.

Measurements were made on the resonant cavity used to modulate the beam to permit calculation of the beam characteristics. Although some discrepancy existed between observed and calculated beam characteristics, the patterns obtained had the expected variation with increasing modulation. The discrepancy is attributed to an error in power measurement.

ACKNOWLEDGEMENTS

The author wishes to thank Professor G.A. Woonton who directed this project. His interest and assistance in the design of the analyser is greatly appreciated. Discussions with him led to a clearer understanding of its operation.

The electron gun, the resonant cavity and the analyser were built under the supervision of Mr. V. Avarlaid, and thanks are due to both Mr. Avarlaid and his staff. The glass-work for the electron gun and vacuum system was done by Mr. R. Lorimer.

Many helpful discussions were held with other members of the Eaton Laboratory. In particular,Mr. Alex Szabo, Mr. Robert Vessot and Mr. Robert Armstrong made valuable contributions to the experiment and to the preparation of this thesis.

This project was supported by Defence Research Board Consolidated Grant DRB 230. The author gratefully acknowledges financial assistance from the Research Council of Ontario in the form of a Scholarship for the period 1953-54, and from the National Research Council in the form of a Studentship for the period 1954-55.

INTRODUCTION

As attempts are made to extend to higher and higher frequencies the range of the electromagnetic spectrum in which useful amounts of power are available, problems arise of both a fundamental and a technological nature. Interest in radiation of wavelengths less than ten centimetres has proceeded from several quarters. Extensive study has been made of microwaves in relation to other parts of the electromagnetic spectrum, the comparison of their nature to that of light being of particular interest. In the field of fundamental physics, wavelengths of several millimetres are employed in studies in microwave spectroscopy but work is handicapped to some extent by limitations in available power. Of a more practical nature, the application of microwaves to communication and radar has resulted in an extremely rapid growth of microwave engineering within the last twenty years.

When tubes of more or less conventional structure were first placed in operation at frequencies in excess of several hundred megacycles per second, a marked deterioration in performance appeared as the frequency was raised. This was traced to electron transit time as the electron passed between the various tube elements. As this transit time became appreciable when compared to one cycle at the signal frequency, results deviated from those at lower operating frequencies. The first corrective measure employed was the obvious one of reducing the size and spacing of the elements in the tube structure to minimize as far as possible transit time effects. Satisfactory operation was thus extended into the decimetre wavelength region but greatly increased difficulties in the fabrication of small tube parts together with the added limitation on the power levels because of small structure sizes, seemed to imply that the technical development of conventional triode and pentode tubes had gone as far as possible.

Additional problems arose with the frequency determining circuit elements externally associated with the tube. The usual combination of inductance and capacitance in the form of a coil and condenser at low frequency cannot be used, as the coil becomes vanishingly small and stray capacity far exceeds that required from elementary considerations at the higher frequencies. This difficulty prompted a closer examination of the assumptions inherent in the use of circuit concepts at radio frequencies and a study of the electromagnetic field quantities involved led Hansen in 1938 to the development of a resonant element for use at microwave frequencies[1]. Essentially the resonator consists of a closed metallic box or cavity in which the storage of electromagnetic energy takes place. A wide variety of geometrical shapes can be used for the cavity, the most practical form being cylindrical or some modification thereon.

A significant advance in the field of high frequency tubes was made in 1939 by the Varian brothers[2] who introduced a device which rather than minimizing electron transit time effects, employed this transit time in the operation of the tube. By passing a beam of electrons through a Hansen type resonator the beam was given a periodic variation in velocity by virtue of its interaction with the electric field within the cavity. As the electrons continued to drift, electrons with higher velocities overtook those travelling at lower velocities and local increases in electron density formed along the beam. The beam then contained a current component at the signal frequency from which output could be derived by means of a second cavity resonator. The principal difference in the operation of this type of tube compared with conventional types is the intermediate process of velocity modulation of the electron beam. Triode and pentode tubes

employ the applied signal to produce current variations immediately, while the high frequency tube uses the signal to cause velocity modulation from which the required current modulation results.

A number of analyses of velocity modulation and the electron bunching process have been made[3-6] with various approximations and under certain assumptions. Some consideration will be given to their significance. A complete analysis which is applicable to beams of high current densities and valid for large modulating signals is not available. To measure electron bunching directly is somewhat difficult and the electron beam characteristics usually must be inferred from a less direct measurement, such as the magnitude of the various harmonic components of current in the beam. This involves the measurement of tube performance under actual operation.

The rate of electron bunch production is equal to the frequency of the applied signal. This establishes bunch durations of the order of 10^{-10} seconds for tubes operating in the microwave range and the measurement of electron density and velocity variations throughout a single bunch is possible only by using an integrated effect due to a large number of bunches. A beam analyser employing this approach has been used successfully by Bloom and Von Foerster[7] and this form of analyser is the subject of this thesis. It operates by displaying on a fluorescent screen electron density and velocity variations in the electron beam during one cycle of the modulation signal. An analyser has been built and used to study a velocity modulated electron beam at an operating frequency of 3000 megacycles. Although some difficulty was experienced in obtaining a sharp trace and small spot size, the patterns obtained show the changes in electron velocity and density as the magnitude of the modulating signal is changed. The results indicate the method of analysis could prove valuable in studying some of the other types of high frequency amplifiers

employing different radio frequency structures and electrode configurations.

I ANALYSIS OF SIMPLE VELOCITY MODULATION AND BUNCHING

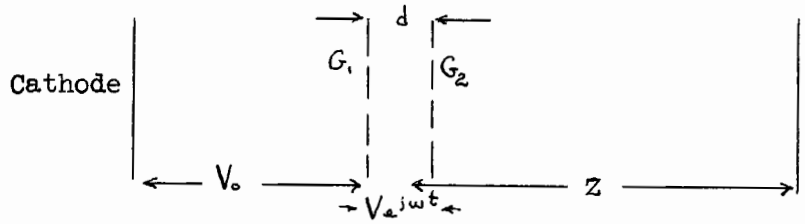

Fig. 1.1 - Diagram for Analysis of Velocity Modulation

The derivation of a simple theory for electron bunching was first done on a purely kinematic basis[3,4]. A uniform beam of electrons is accelerated through a potential V_o and is allowed to pass through a resonant cavity with grids G_1 and G_2 separated a distance d. A modulating voltage $Ve^{j\omega t}$ appears across the gap where V is positive if it accelerates the electrons. The electric field between the grids in the region of the electron beam is assumed to be uniform and given by $Ve^{j\omega t}/d$. Applying Newton's second law relating force and acceleration

$$F = ma$$

we have for the electron during its passage through the cavity

$$m \frac{dv}{dt} = e E e^{j\omega t}$$

If v_o is the initial electron velocity and v its final velocity

$$v - v_o = \frac{eV}{md} \int_{t_1'}^{t_2'} e^{j\omega t} \, dt$$

where the limits of the integral are the times at which the electron enters and leaves the gap d. The assumption is now made that $t_2' - t_1'$ does not deviate greatly from the transit time for an electron of constant velocity v_o

$$t_2' - t_1' = d/v_o$$

On performing the integration and noting that the initial velocity v_o

is related to the accelerating potential V_o by the energy relation

$$\frac{1}{2} m v_o^2 = e V_o$$

the velocity on exit from the cavity is

$$v = v_o \left\{ 1 + \frac{V}{2V_o} M e^{j(\omega t_2' - \theta/2)} \right\}$$

where θ is the transit angle for the electron

$$\theta = \omega(t_2' - t_1')$$

and the beam coupling coefficient M is defined

$$M = \frac{\sin \theta/2}{\theta/2}$$

For zero transit angle the beam coupling coefficient M = 1 and the maximum effect of the gap voltage V is experienced by the electron. For $\theta \simeq 0$ we have M smaller than unity and the effective modulating voltage is less than V. This is a consequence of the fact that the field and therefore the force on the electron is not constant as the electron crosses the gap. The effective phase of the modulating signal is approximately that when the electron is at the centre of the gap. In further analysis we will let the time the electron passes the gap centre be t_o.

Webster[3] has studied the behaviour of a velocity modulated electron beam as it moves beyond the resonant cavity. At a point a distance Z from the gap centre the arrival time t_1 of an electron can be related to the departure time t_o by

$$\omega t_1 = \omega t_o + \theta_o - X \sin \omega t_o \qquad (1.1)$$

where ωt_o is the effective modulating phase

θ_o is the drift space transit angle for the unmodulated electron beam

X is called the bunching parameter and is defined

$$X = M \frac{ZV\omega}{2V_o v_o}$$

Equation 1.1 is plotted in Figure 1.2 for different values of the bunching parameter. For X less than unity there is a single valued relation between the time an electron arrives at a given point and the time it left the point of modulation. As X increases and takes on values greater than one however, the function is no longer single valued and it is possible to have electrons that left the cavity at different times all arrive at the same time at Z. This can happen if at one time electrons in the beam are slowed down and at a later time others are increased in speed sufficiently to overtake the earlier electrons as they reach point Z. The figure also illustrates the fact that these faster electrons can pass the slower ones to arrive at Z before them. After this crossing of trajectories occurs the nature of the electron beam has changed in that the velocity of electrons at one point can have as many as three values simultaneously.

The crossing of electron trajectories has a further consequence of causing infinite peaks in the beam current as seen in Figure 1.3 which is a plot of Webster's relation for beam current

$$I = \frac{I_o}{1 - X \cos \omega t_o} \qquad (1.2)$$

where I_o is the D.C. beam current. It is seen that the current peaks in Figure 1.3 occur just at the times the slope of the curves in Fig. 1.2 becomes infinite. At this time electrons that left the modulation plane during a finite increment of time arrive at Z together in a zero time increment.

From equation 1.2 it can be seen that the bunching parameter must be equal to or greater than unity to have the infinities of current appear. For a given value of X the peaks are due to electrons having modulation phases

$$\omega t_o = \pm \cos^{-1} \frac{1}{X}$$

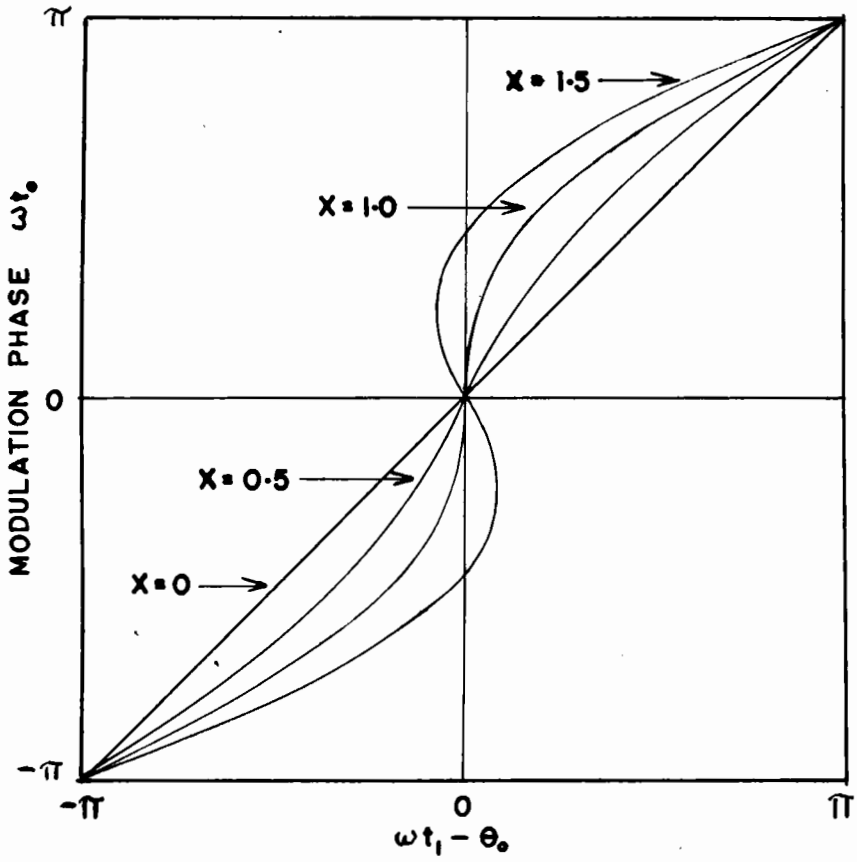

FIG. 1·2 MODULATION AND ARRIVAL PHASES FOR VARIOUS BUNCHING PARAMETERS

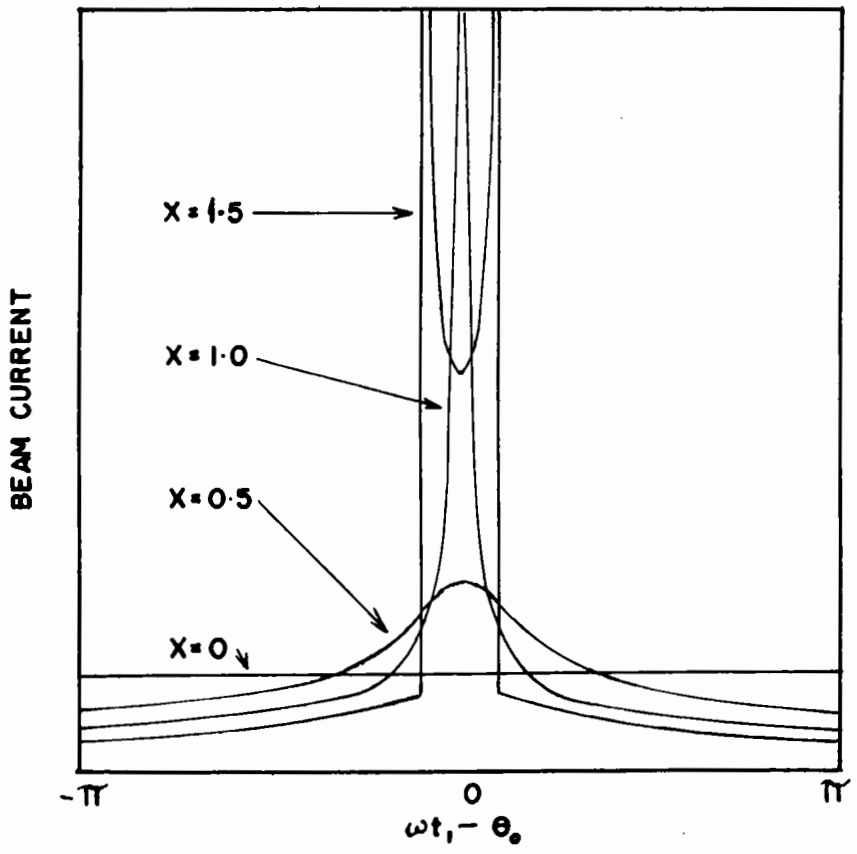

FIG. 1·3 BEAM CURRENT AS A FUNCTION OF ARRIVAL PHASE

and by using equation 1.1 the separation in arrival phase between the two peaks is

$$\phi = 2(\sqrt{X^2 - 1} + \cos^{-1} \frac{1}{X}) \qquad (1.3)$$

The electron velocity will be triple valued between the arrival phases at which the peaks occur and single valued outside of these phases.

II THE HIGH FREQUENCY DEFLECTION SYSTEM

To determine the nature of the bunches formed as the velocity modulated electron beam travels along the drift space, the beam is passed through a deflection system that sweeps it in a circular path. The circle appears on a fluorescent screen placed to intercept the beam. Density variations appear as intensity variations on the screen while velocity variations appear as a change in the radial position of the beam at the given point of phase. The deflection system is driven by the same signal source as is used to produce the velocity modulation. This establishes perfect synchronism between scanning and bunch production and a stationary pattern appears on the screen. The effect of changing the magnitude of the modulating voltage is visible as a change in the screen trace.

The deflection system which produces the circular trace consists of two sets of Lecher wires placed at right angles and positioned for the beam to pass through the region where they cross. A voltage standing wave maximum is caused to appear at the point where the electron beam passes between one of the Lecher wire pairs by using a resonant half wave section terminated by a short circuit.

In examining the deflection characteristics of a single Lecher wire pair, the finite transit time of an electron must be considered. It will be assumed however that the electron in passing between the wires does not deviate from its path until it has reached a point where the deflection system has no longer any significant effect on it. The finite propagation velocity of the field around the Lecher wires will be ignored and the problem explored using an electrostatic solution for the field between the wires. With the electron velocities employed in the experiment

approaching one-fifth of the velocity of light, the approximation concerning the velocity of propagation of the electric field may not be completely justified.

For two parallel cylindrical conductors of radius R and centre to centre spacing 2d having a potential difference of V_D existing between them

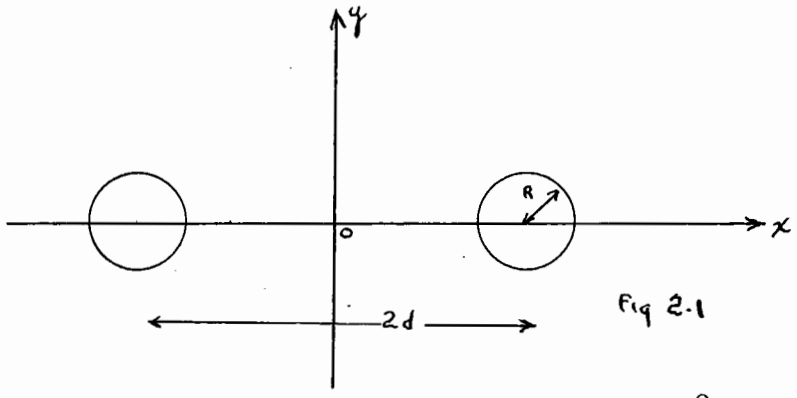

Fig 2.1

the potential at any point in the xy plane is defined from[8]

$$\phi = \frac{V_D}{2} \frac{\ln\left[(x-a)^2 + y^2\right] - \ln\left[(x+a)^2 + y^2\right]}{\ln\left[d-R-a\right]^2 - \ln\left[d-R+a\right]^2} \qquad (2.1)$$

where

$$a = \sqrt{d^2 - R^2}$$

If it be assumed that the electron trajectory is confined to the y axis it is possible to calculate the gain in the momentum of an electron as it passes between the pair of wires.

Differentiating ϕ with respect to x to find the deflection field and putting x = 0, then:

$$E_x = -\frac{V_D}{2} \cdot \frac{4a}{y^2 + a^2} \cdot \frac{1}{\ln G}$$

where

$$G = \left\{\frac{d - R + a}{d - R - a}\right\}^2$$

The electron momentum in the x direction can be integrated from this

expression. If ωt is the phase of the voltage across the wire pair when an electron is at the co-ordinate origin then

$$mv_x = \frac{2V_D ae}{v_y \ln G} \int_{-\infty}^{\infty} \frac{\cos(\omega t - y/v_y)}{y^2 + a^2} \, dy$$

where the electron has velocity components v_x and v_y and t has been replaced by y/v_y in the momentum-force relation. The infinite limits have been used on the integral as the field falls off rapidly on either side of the wire pair. Evaluating the integral[9] gives

$$mv_x = \frac{2V_D ae}{v_y \ln G} \cdot \frac{\pi}{a} e^{-\omega a/v_y} \cos \omega t$$

The tangent of the angle of deflection θ measured from the centre line is then:

$$\tan\theta = \frac{v_x}{v_y} = \frac{2e/m \; V_D \pi}{v_y^2 \ln G} e^{-\omega a/v_y} \cos \omega t$$

$$= \frac{V_D}{V_o} \cdot \frac{\pi}{\ln G} e^{-\omega a/v_y} \cos \omega t \qquad (2.2)$$

The deflection of the electron beam varies sinusoidally at the signal frequency.

The exponential variation of the deflection is a consequence of the field variation with y. It differs from the deflection produced by two parallel plates. The reason for this can be made clear by the following qualitative argument. For an electron deflected by two parallel plates of finite length and spacing, a uniform field localized between the plates being assumed, signal frequencies exist at which the electron deflection is zero. For these frequencies the transit time through the deflection field is a multiple of the signal period and deflections in one direction exactly cancel those in the other. An infinite number of such frequencies exist, related harmonically to the frequency whose period is just equal to the

transit time.

For an electron deflected by a wire pair, the result is somewhat different. The form of the electric field about the wire pair results in a variation in magnitude of the force acting on the electron at different points along its path. The only condition permitting a resultant deflection of zero is that for which the deflection voltage just changes sign as the electron crosses the centre of the system. The force experienced by the electron is plotted in Fig. 2.2(a). The positive and negative contributions just balance out. The maximum electron deflection occurs when the peak deflection voltage appears across the wires as the electron crosses the centre of the system. Figure 2.2(b) illustrates this situation and the positive contributions exceed the negative ones to produce a net deflection. The cause of the exponential variation can be seen by studying the effect of a larger number of changes in direction of the deflection field along the electron path. This can be brought about by increasing the deflection signal frequency or decreasing the electron velocity in the y direction. In Figure 2.2(c) the positive and negative contributions are now more nearly equal and the net positive effect is smaller than that of Figure 2.2(b). That the exact form of the variation is an exponential function cannot be directly inferred from the above reasoning but this qualitative argument indicates that the analytical result is reasonable.

If the angle of maximum deflection is examined as a function of beam voltage V_o

$$\tan\theta = \frac{V_D}{V_o}\frac{\pi}{\ln G}\exp\left[\frac{-\pi c a}{\lambda}\sqrt{\frac{2m}{e}}\frac{1}{\sqrt{V_o}}\right]$$

$$= \frac{V_D}{V_o}\frac{\pi}{\ln G}\exp\left[-2\sqrt{\frac{V_m}{V_o}}\right] \qquad (2.3)$$

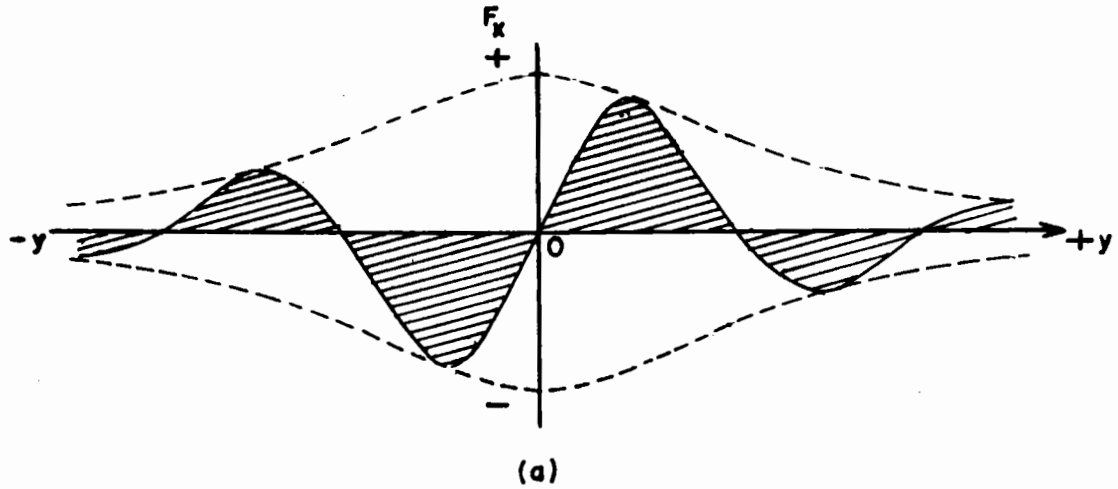

(a)

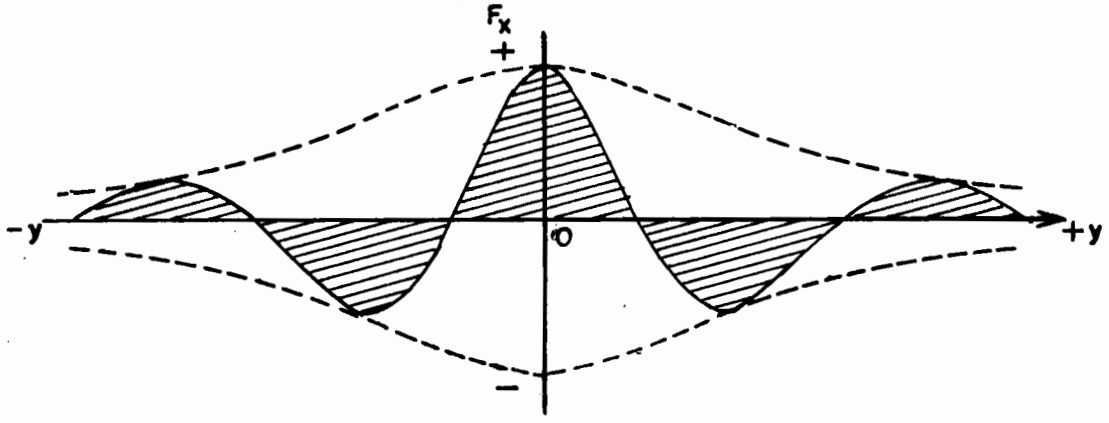

(b)

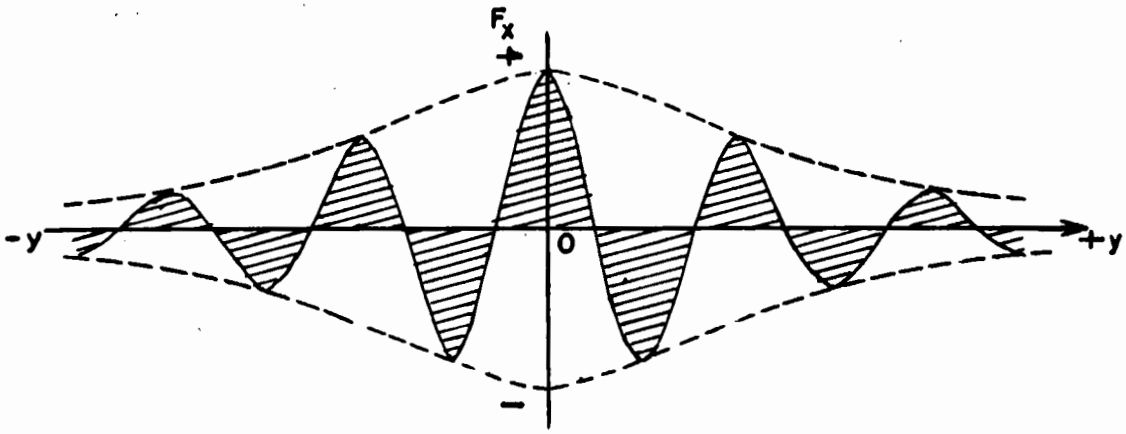

(c)

FIG. 2·2 VARIATION OF FORCE ON AN ELECTRON ALONG ITS PATH

where c is the velocity of light and λ the free space wavelength. The quantity V_m is defined by:

$$V_m = \frac{\pi^2 c^2}{2e/m} \frac{a^2}{\lambda^2}$$

$$= 2.521 \times 10^6 \frac{a^2}{\lambda^2} \text{ volts}$$

By differentiating (2.3) with respect to V_o it can be shown that for a given deflection voltage across the wires the maximum deflection of the electron beam will occur for an accelerating voltage V_o equal to V_m. Equation 2.3 is in agreement with the form indicated by Bloom and Von Foerster[7].

In the deflection system for beam analysis are two Lecher wire pairs placed at right angles. Let the distance from the centre of one pair to the centre of the other pair be s. By properly phasing the voltages appearing across each set it is possible to produce a circular trace on the screen of radius $R = l \tan \theta$ where l is the distance from the analyser to the screen. Von Foerster has studied the variation in the form of the circular trace resulting from small variations in beam velocity as would occur in velocity modulation. He found that the system exhibits a radial sensitivity to velocity variations defined by

$$\frac{dR}{dV} = -\frac{R_o}{V_o}\left\{1 - \left[\frac{\frac{1}{4}\sqrt{V_s}\cos 2\phi + \sqrt{V_m}}{\sqrt{V_o}}\right]\right\} \qquad (2.4$$

where R_o is the radius of the undisturbed circle

V_s is the beam voltage required for an electron to have a transit angle of π in crossing the distance s between the Lecher wire pairs.

$$V_s = 1.008 \times 10^7 \frac{s^2}{\lambda^2} \text{ volts}$$

ϕ is the azimuthal angle measured around the circular trace from a line bisecting the right angle formed by the Lecher wire pairs; the origin of co-ordinates being the position of the spot due to the undeflected beam. The co-ordinate system and its relation to the Lecher wire pairs is shown in Figure 2.3.

To describe the performance of a system, a velocity sensitivity parameter can be defined

$$\delta = -\frac{dR}{dV}\frac{V_o}{R_o}$$

$$= 1 - \frac{\frac{1}{4}\sqrt{V_s}\cos 2\phi + \sqrt{V_m}}{\sqrt{V_o}}$$

It ranges in value between

$$\delta_o = 1 - \sqrt{\frac{V_m}{V_o}} - \frac{1}{4}\sqrt{\frac{V_s}{V_o}} \qquad (2.5a)$$

$$\delta_{\pi/2} = 1 - \sqrt{\frac{V_m}{V_o}} + \frac{1}{4}\sqrt{\frac{V_s}{V_o}} \qquad (2.5b)$$

As the choice of V_m has a strong control on the geometry of a single Lecher wire pair its value is governed by practical considerations of wire size and centre to centre spacing. The magnitude of V_s is determined only by the spacing between the sets of Lecher wire pairs. By increasing this spacing the sensitivity can be made as large as desired, subject only to the limitation that the electron should not have deviated greatly from the axis as it passes between the second pair of Lecher wires. This restriction is necessary in order that the electron pass between the wires at the maximum of a voltage standing wave. The value of δ for V_o = 10,000 volts and V_o = 2,000 volts is plotted in Figure 2.3 for the

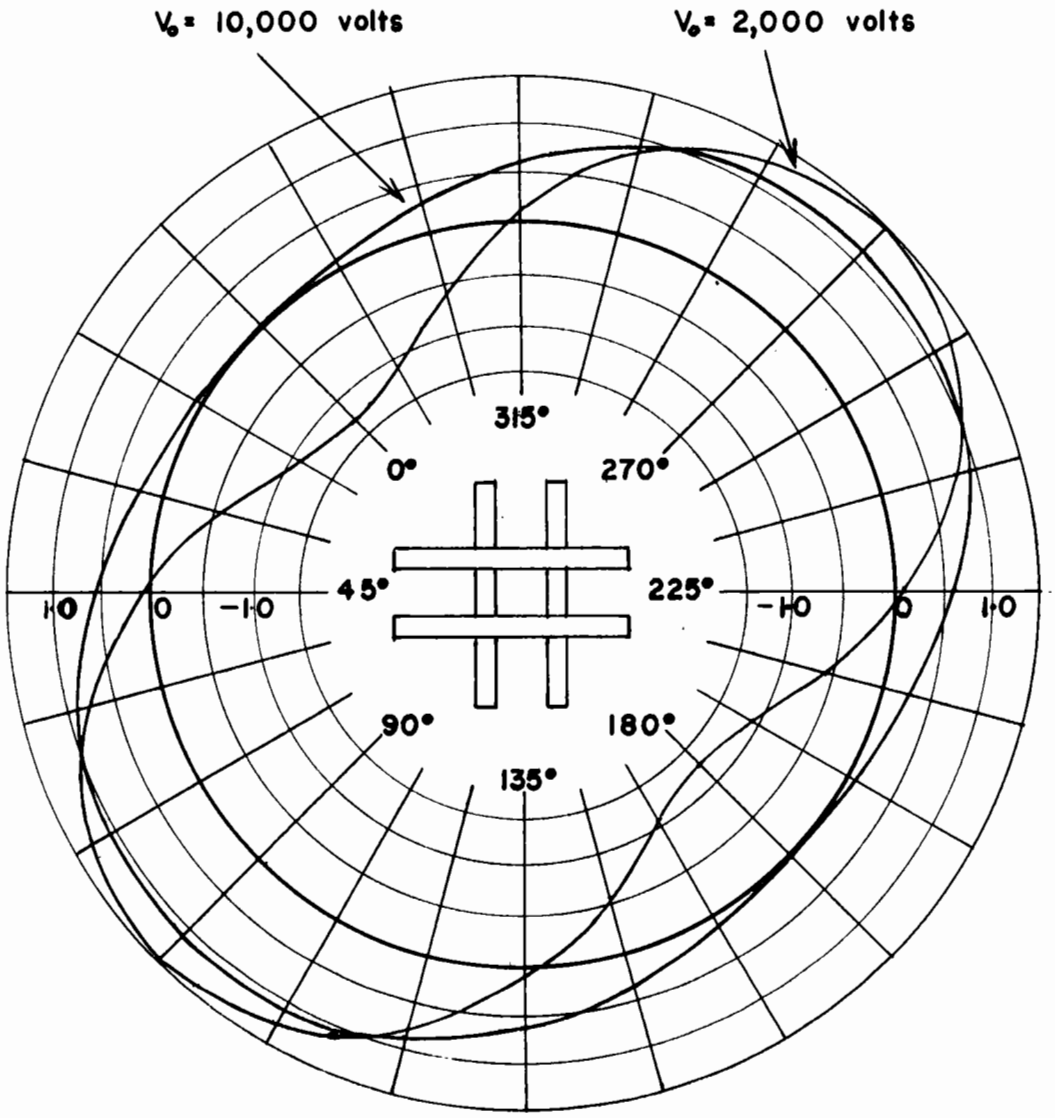

FIG. 2·3

VELOCITY SENSITIVITY PARAMETER AS A FUNCTION OF AZIMUTHAL ANGLE

V_m = 1,515 volts

V_s = 59,740 volts

geometry employed in the experiment. For a 10,000 volt beam the velocity sensitivity parameter varies between 0 and 1.22. With traces of 2.1 cm diameter the maximum sensitivity is 780 volts/mm. There are two points on the curve where the velocity sensitivity is zero. At these points all electrons have the same radial position for beam voltages in the region of 10,000 volts.

III THE EXPERIMENT

A block diagram of the experiment is shown in Figure 3.1. An electron beam passes through a resonant cavity which is excited by a 10 cm. signal. The voltage variations across the gap of the cavity cause velocity modulation of the beam. After drifting in a field free region the beam passes through the two pairs of Lecher wires which form the analyser. The deflected beam finally impinges on a 5" fluorescent screen to form the pattern. The radio frequency energy to drive the resonant cavity and deflection system is supplied by a 10 cm magnetron.

1. Experimental Equipment

The magnetron is a Research Enterprises Limited Type 3DX and is used with a modulator built by the Radio and Electrical Engineering Division of the National Research Council. It operates at a signal wavelength of 10.00 cm. as measured by a Polytechnic Research and Development Company Type 583-C cavity wavemeter. The magnetron is pulsed for a period of 1.0 μsec. at a repetition rate of 1072 pulses per second.

The electron gun is shown in Figure 3.11. The gun cathode is pulsed with a 1.0 μsec. 450 volt negative pulse. During the pulse "off" period a retarding field exists between the cathode and anode and the electron beam is suppressed. A single timing source is used for both the magnetron and electron gun pulses in order that they occur simultaneously.

The timing circuit is shown in Figure 3.2. It employs a type 2D21 tetrode thyratron to produce trigger pulses of very short duration.

The pulse repetition frequency is controlled by varying the control grid voltage of the 2D21. The circuit constants permit adjustment from 1000-2200 p.p.s. A type 12AU7 tube is used as a cathode follower to provide an output to trigger the magnetron modulator. The trigger amplitude exceeds

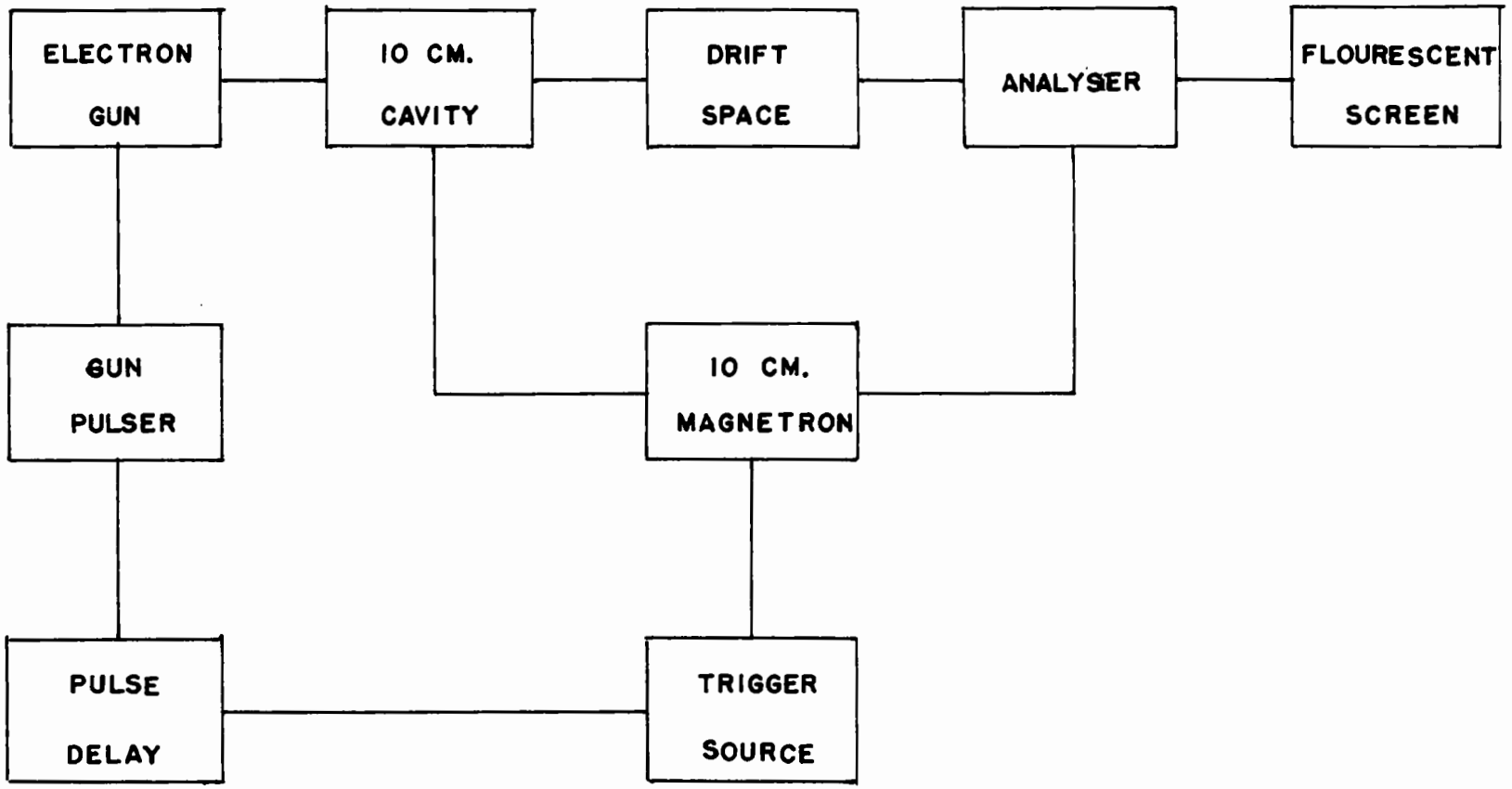

FIG. 3·1 BLOCK DIAGRAM OF EXPERIMENTAL SETUP

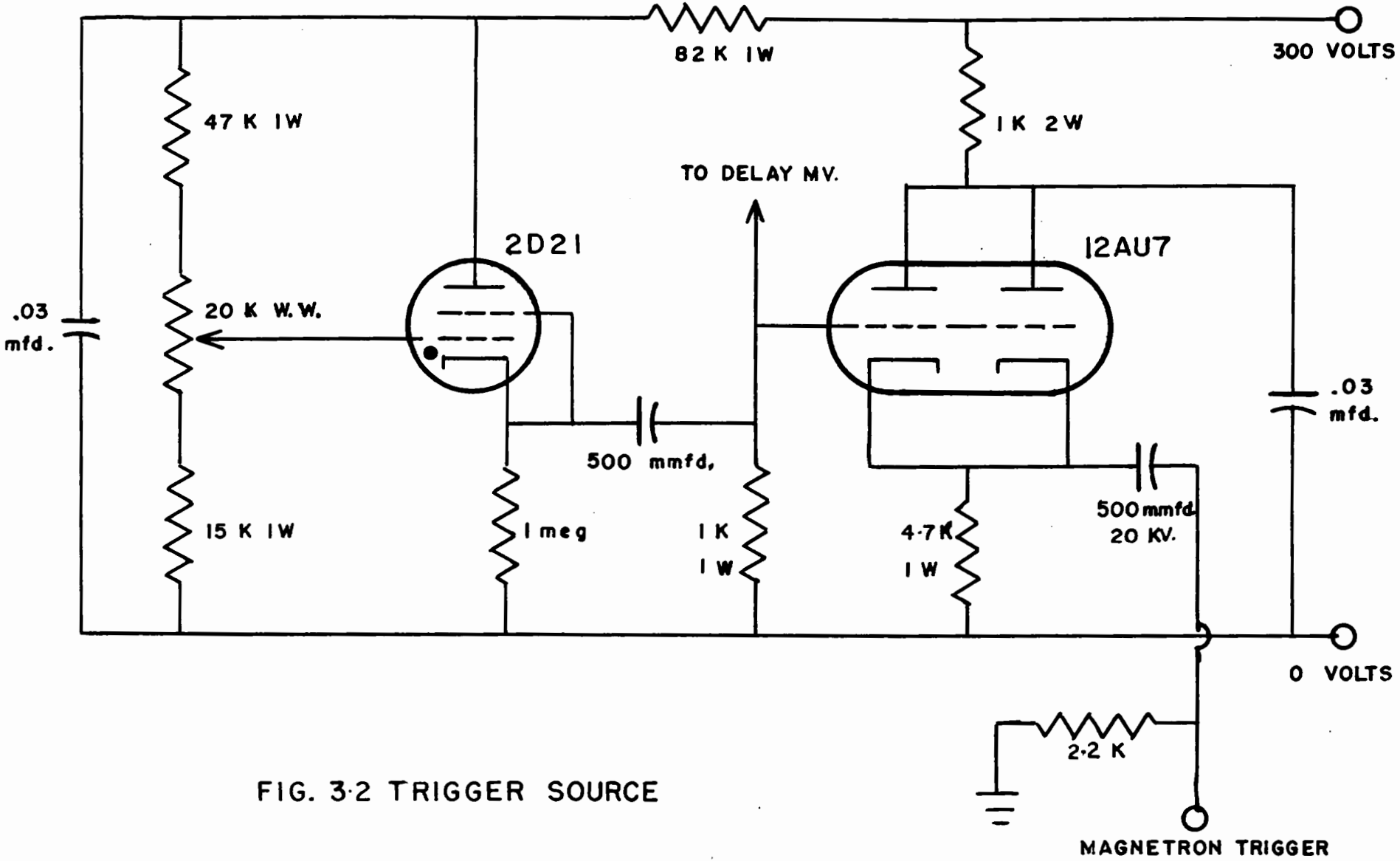

FIG. 3·2 TRIGGER SOURCE

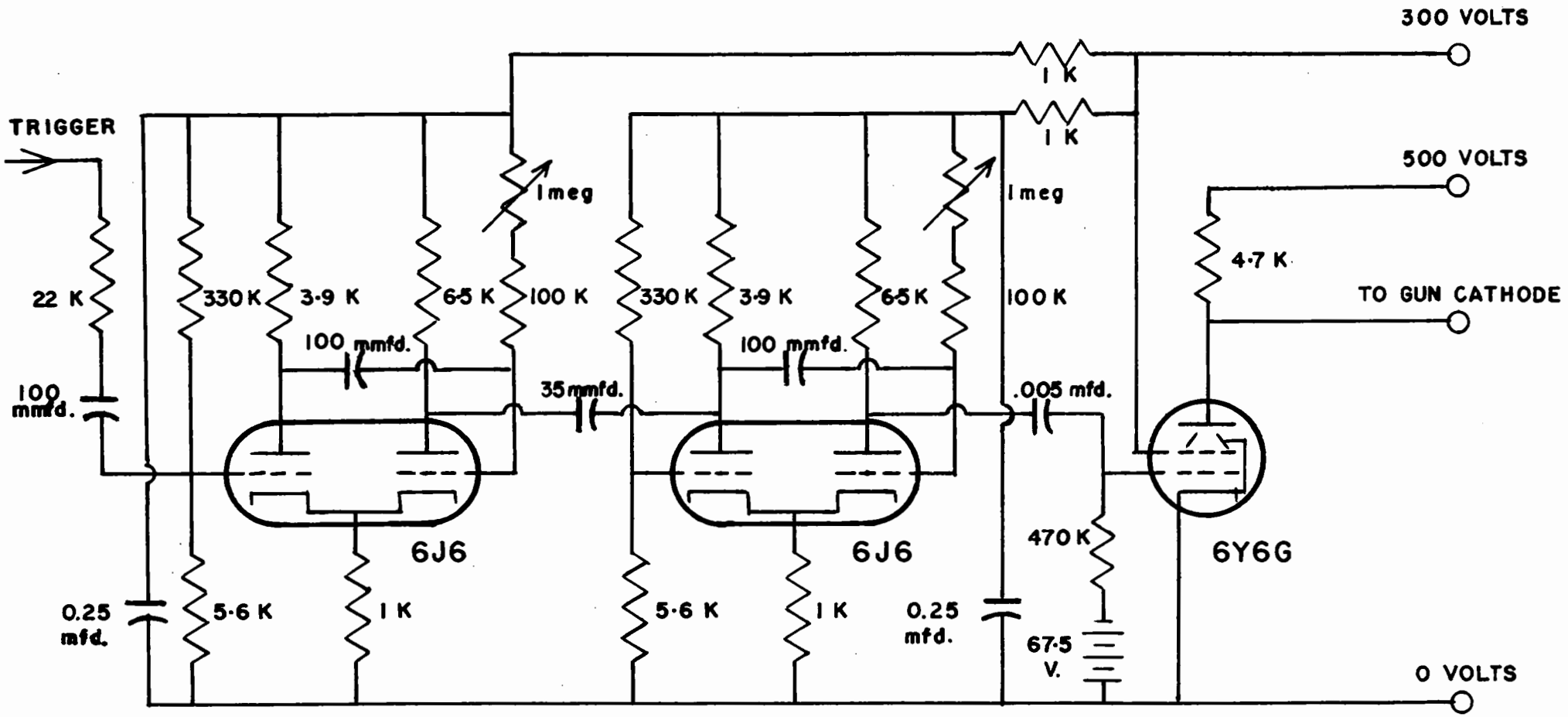

FIG. 3.3 DELAY UNIVIBRATOR AND GUN PULSER

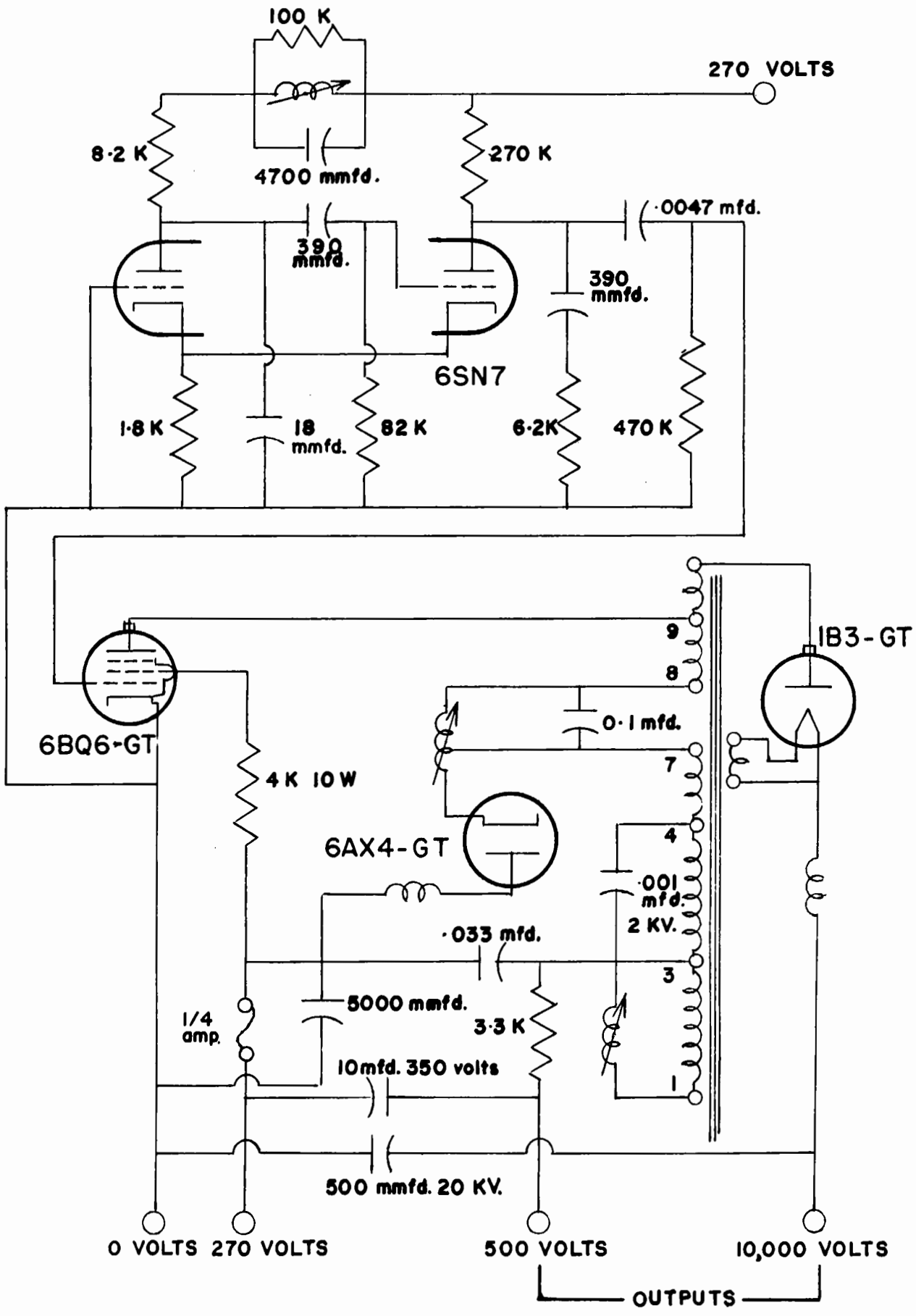

FIG. 3·4 HIGH VOLTAGE POWER SUPPLY

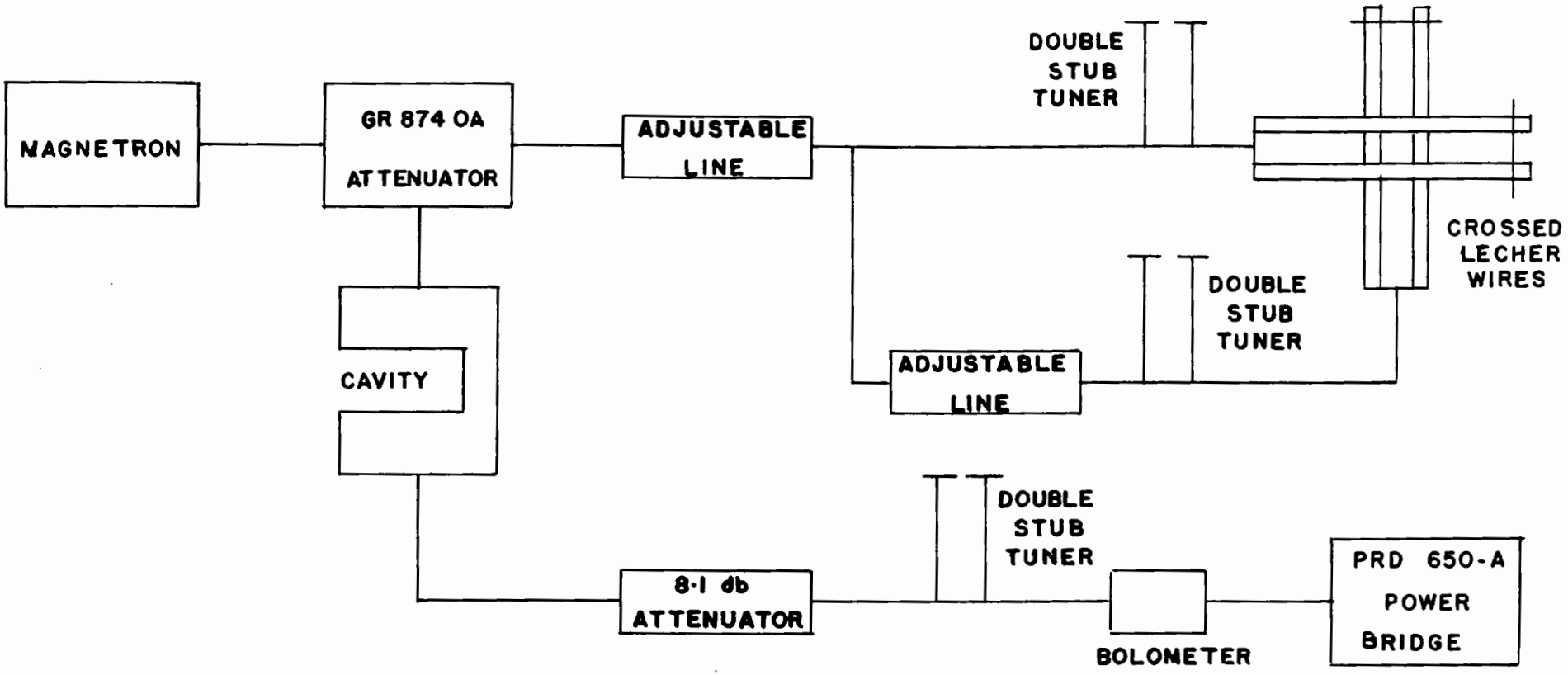

FIG 3·5 BLOCK DIAGRAM OF RADIO FREQUENCY CIRCUIT

50 volts which is more than adequate for reliable modulator operation. A 20 kilovolt 500 mmfd. isolating condenser is used in the trigger line as the trigger chassis and the magnetron modulator differ in potential by the full beam accelerating voltage.

It was determined that there was a 1.6 μsec. delay between the application of the trigger to the modulator and the magnetron output pulse. The voltage pulse to the electron gun is delayed by a similar interval.

The circuit for generating the voltage pulse to the electron gun is shown in Figure 3.3. It consists of two univibrators in cascade driving a type 6Y6 tube to provide a 450 volt negative pulse for the electron gun cathode. The pulse delay is variable between 1 and 3 μsec. and the pulse length is variable between 1 and 9 μsec. This control is achieved by providing adjustable time constants in the univibrator circuits.

The final voltage for accelerating the electron beam is provided by a television type high voltage supply. The circuit is shown in Figure 3.4. In addition to a 10,000 volt output there is a 500 volt source which is used as the plate supply for the 6Y6 pulser tube.

The radio frequency circuit is shown in Figure 3.5. The magnetron feeds power to the cavity through a GR Type 874 OA cut-off attenuator. This permits easy adjustment of cavity power and therefore of cavity gap voltage. An adjustable line between the magnetron and the deflection system permits adjustment of the scanning signal phase relative to the cavity gap voltage. An additional line stretcher between the Lecher wire pairs makes it possible to establish the required phase difference for a circular trace.

2. The 10 Cm. Cavity

The resonant cavity is a capacitively loaded coaxial type and was designed from the curves of W.W. Hansen[10]. A gridless form is used to avoid the production of secondary electrons from grid wires. Calculations

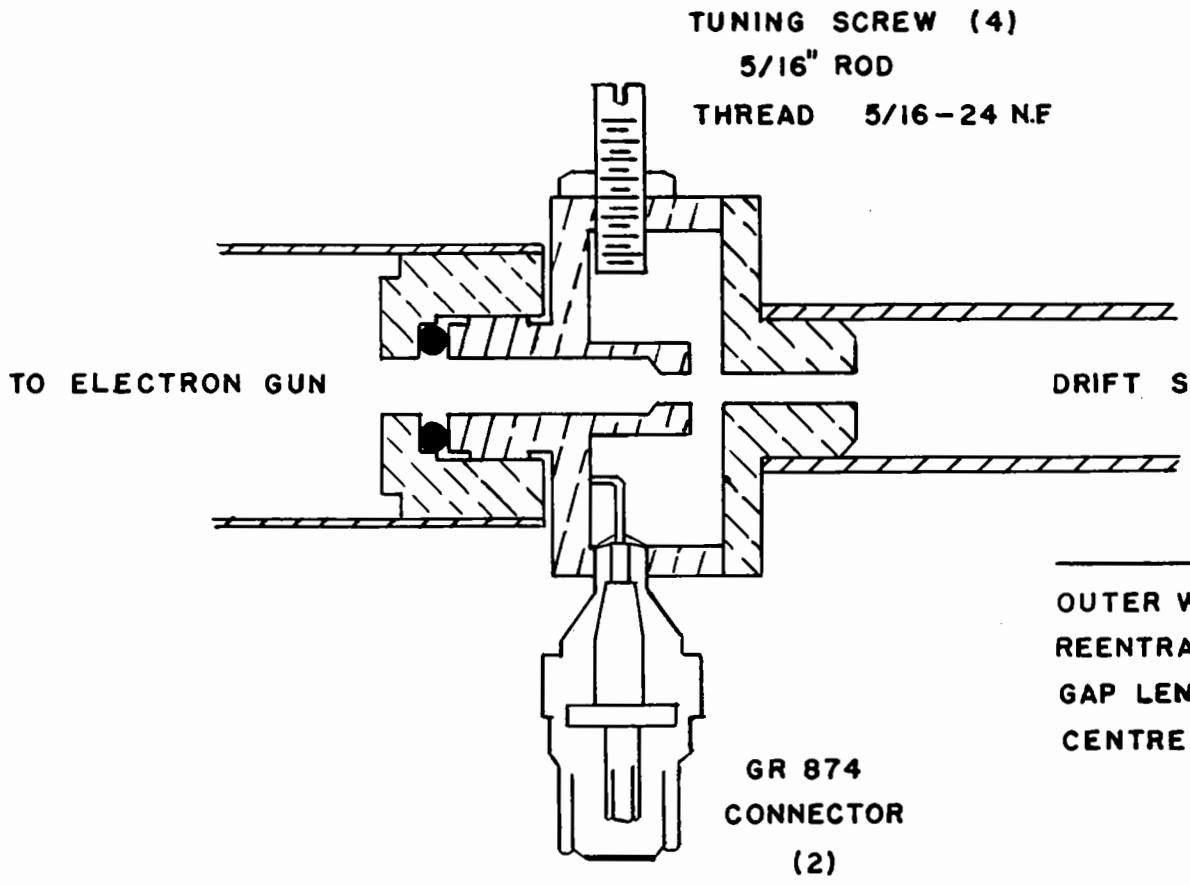

CAVITY DIMENSIONS

OUTER WALL DIAMETER	4·20 CM.
REENTRANT POST DIAMETER	1·20 CM.
GAP LENGTH	0·45 CM.
CENTRE HOLE DIAMETER	No. 17 DRILL

FIG. 3·6 10 CM. RESONANT CAVITY DETAILS

were made on the basis of a gridded gap of 5.0 mm. The actual gap was reduced to 4.5 mm. This maintains the same capacity across the gap when the area of the capacitor plates formed by the gap is reduced by the introduction of the central hole. Tuning screws are provided to resonate the cavity at the magnetron frequency. The cavity details are shown in Figure 3.6.

The operation of the bunching cavity is determined by three parameters; - the resonant frequency ω_o, the unloaded Q or Q_o and the shunt resistance R_s measured along the cavity axis as traversed by the electron beam.

The resonant frequency is adjusted by altering the cavity volume. Four tuning screws are located in the region of the cavity where the energy storage is principally in the form of a magnetic field. In such a region a decrease in volume results in an increase in the resonant frequency of the cavity. The cavity was resonated at the magnetron frequency before installation into the vacuum system. This is permissible as the electron beam used provides very little loading. The tuning screws were then sealed.

The unloaded Q of a cavity is defined as:

$$Q_o = \frac{\omega_o W}{P_c}$$

where W is the energy stored in the cavity and P_c is the power dissipated by the cavity. The internal impedance of any source used to excite the cavity results in the dissipation of additional power. A Q factor can be defined relating the dissipation of power external to the cavity to the energy stored in the cavity:- $Q_1 = \omega_o \frac{W}{P_1}$

where P_1 is the power dissipated external to the cavity in the internal impedance of a power source or in a load placed on the cavity.

The determination of cavity Q requires the measurement of the variation of the input impedance of the cavity as a function of frequency. Changes in input impedance appear as a variation in the standing wave ratio on the input line. The test setup is shown in Figure 3.7.

Slater has examined the variation of input standing wave ratio and the power coupled to the cavity at frequencies in the region of resonance

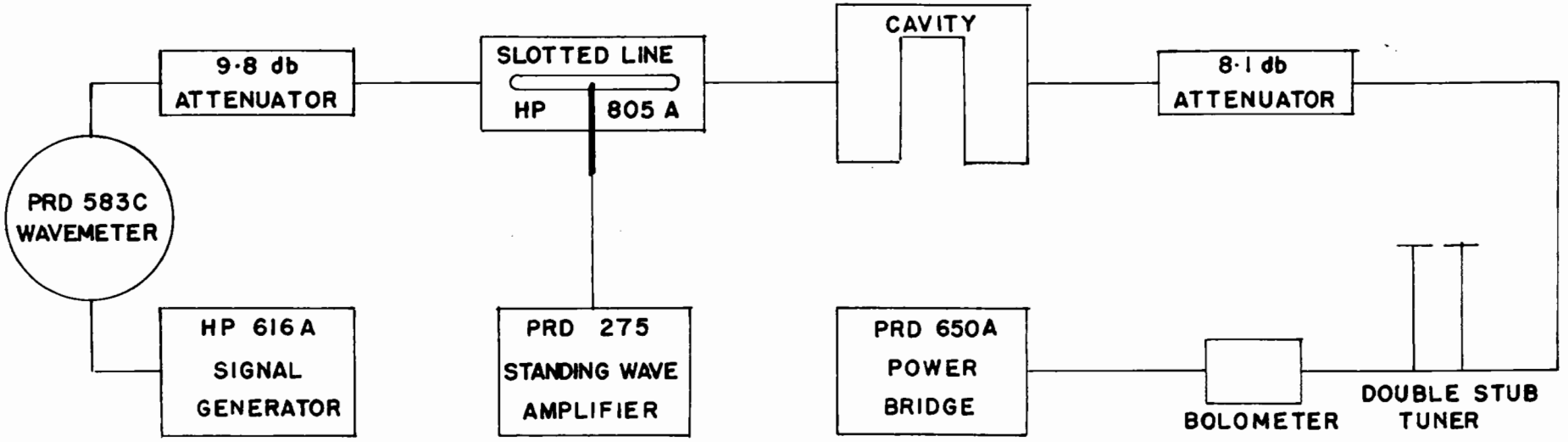

FIG. 3·7 BLOCK DIAGRAM OF CAVITY MEASUREMENT SETUP

for a cavity with a single coupling loop. These are expressed in terms of Q_o and Q_1; the power dissipation in the driving source impedance being associated with Q_1. At resonance the input standing wave ratio is defined by

$$\sigma_o = Q_o/Q_1 \tag{3.1}$$

where for

$$Q_o/Q_1 > 1 \qquad \sigma_o = \text{V.S.W.R.}$$

$$Q_o/Q_1 < 1 \qquad \sigma_o = 1/\text{V.S.W.R.}$$

The former case represents overcoupling and the latter undercoupling. It is assumed that losses in the coupling loop are small.

Slater showed that at frequencies $\Delta\omega$ from the resonant frequency ω_o such that the standing wave ratio is equal to

$$r_1 = \frac{1 + \sigma_o + \sqrt{1+\sigma_o^2}}{1 + \sigma_o - \sqrt{1+\sigma_o^2}} \tag{3.2}$$

the value of $\Delta\omega$ satisfies

$$2\frac{\Delta\omega}{\omega_o} = \frac{1}{Q_1} + \frac{1}{Q_o} = \frac{1}{Q_L} \tag{3.3}$$

where Q_L is called the loaded Q of the system. Therefore a measurement of the input V.S.W.R. at resonance and the frequencies at which the V.S.W.R. has the value defined by equation 3.2 permits the determination of the unloaded cavity Q as well as the total loaded Q.

The ratio of the power coupled to the cavity to that delivered by the same generator driving a matched resistive load is given by[11]

$$\frac{P}{P_o} = \frac{4/Q_o Q_1}{\left(\frac{\omega}{\omega_o} - \frac{\omega_o}{\omega}\right)^2 + \left(\frac{1}{Q_o} + \frac{1}{Q_1}\right)^2} \tag{3.4}$$

where P is the power coupled to the cavity and P_o that coupled to a matched load.

The analysis which has been given for a cavity with a single coupling loop can be extended to that for two coupling loops by replacing the power dissipation associated with Q_o by that associated with Q_o and the power dissipated in the load impedance on the output coupling. If the Q factor associated with the power dissipated in this load impedance is defined as Q_2 then:-

$$\frac{1}{Q_o} \text{ is replaced by } \frac{1}{Q_o} + \frac{1}{Q_2} = \frac{1}{Q_o'}$$

$$Q_o' = \frac{Q_o Q_2}{Q_o + Q_2}$$

At resonance with a load in line 2 the V.S.W.R. (or its reciprocal) on the input line is obtained by replacing Q_o by Q_o' in (3.1).

$$\sigma_{o1} = \frac{1}{Q_1} \frac{Q_o Q_2}{Q_o + Q_2}$$

If the coupling parameters are defined

$$\gamma_1 = Q_o/Q_1$$

$$\gamma_2 = Q_o/Q_2$$

then

$$\sigma_{o1} = \frac{\gamma_1}{1 + \gamma_2} \qquad (3.5a)$$

If terminal 1 is loaded and the cavity driven from terminal 2, the V.S.W.R. (or its reciprocal) in line 2 is

$$\sigma_{o2} = \frac{\gamma_2}{1 + \gamma_1} \qquad (3.5b)$$

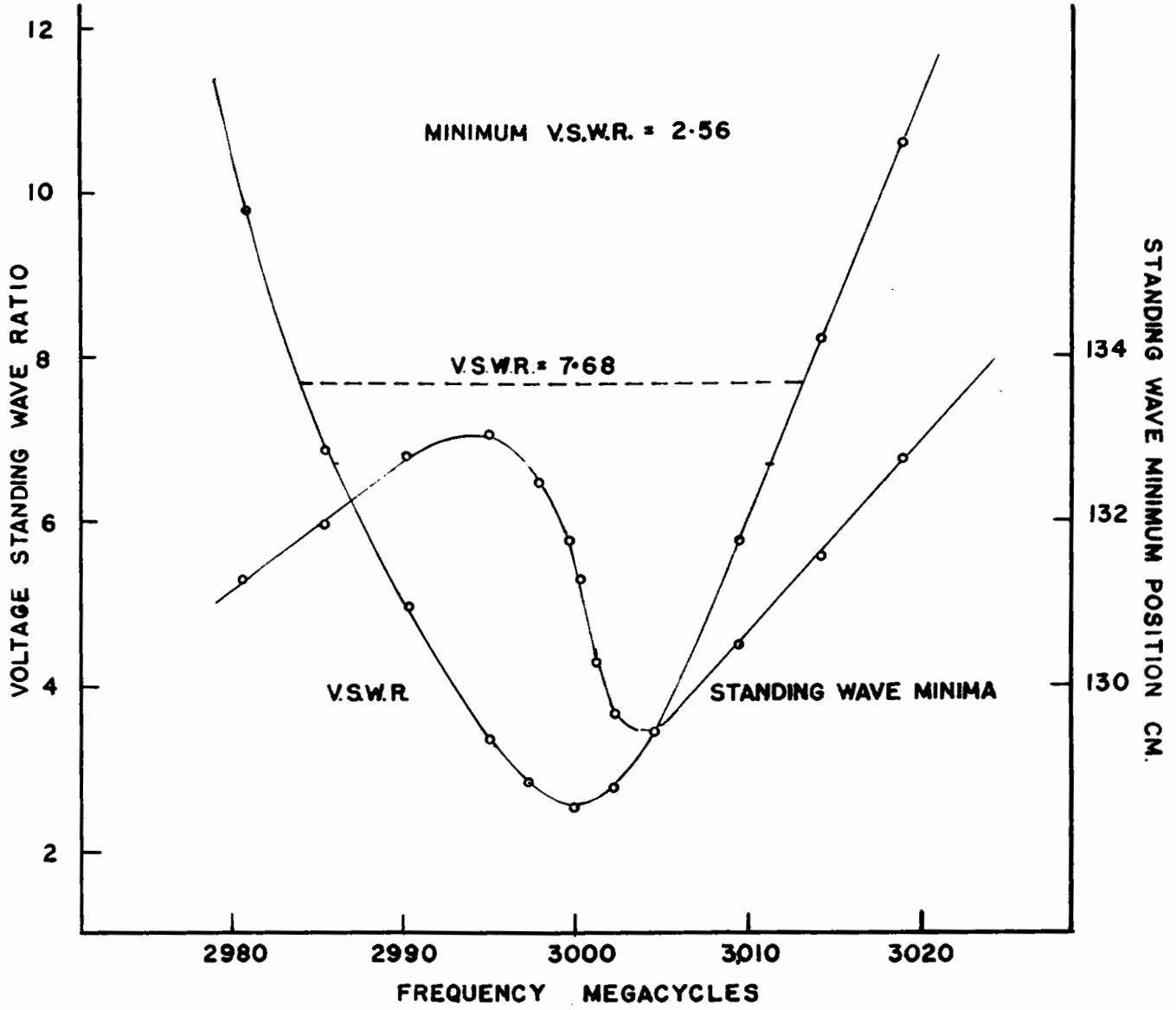

FIG. 3·8 INPUT VOLTAGE STANDING WAVE RATIO AS A FUNCTION OF FREQUENCY — INPUT TO No. 1

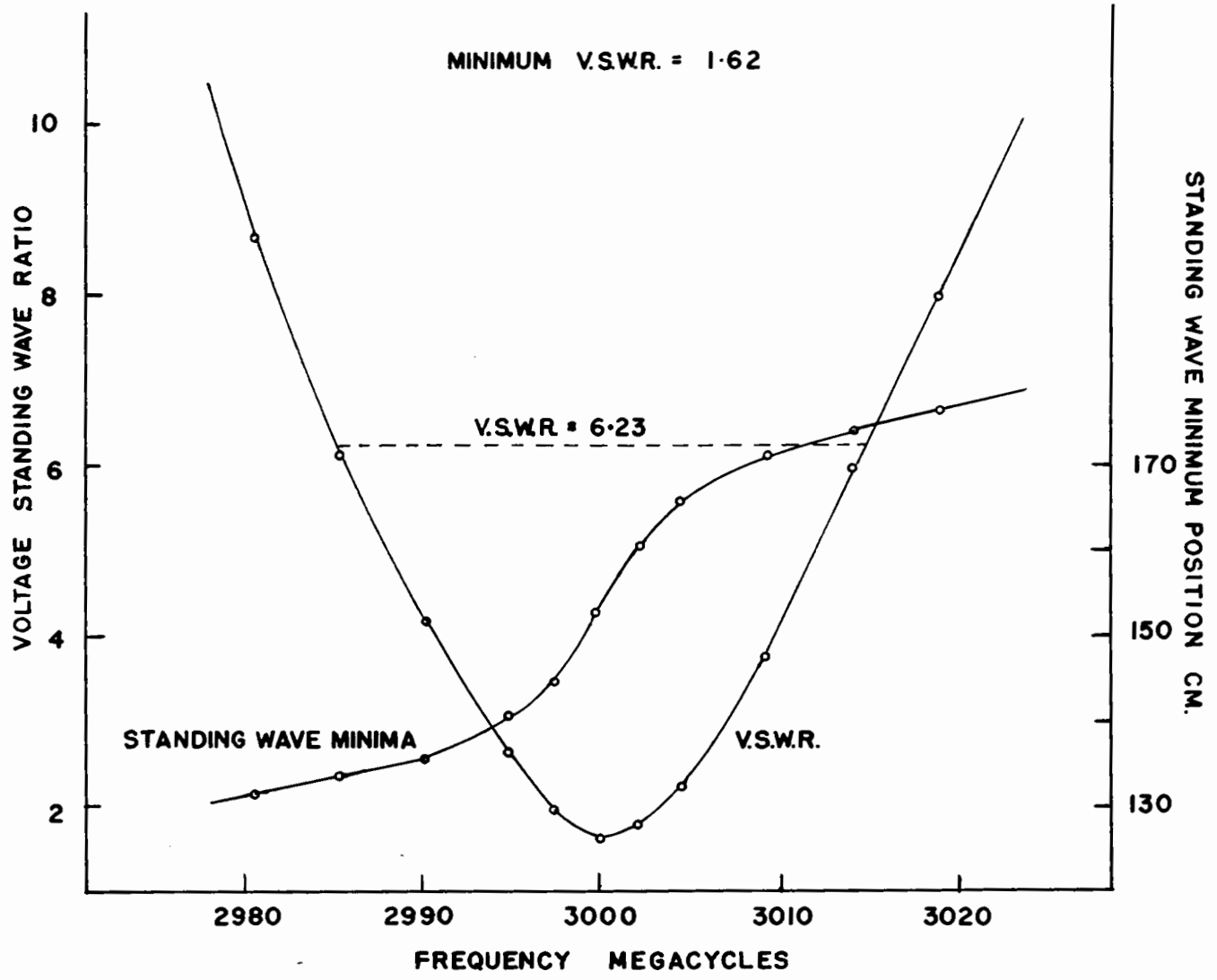

FIG. 3·9 INPUT VOLTAGE STANDING WAVE RATIO AS A FUNCTION OF FREQUENCY — INPUT TO No. 2

where both the source and load are matched attenuators providing non-reflecting terminations.

Equations 3.2 and 3.3 are still applicable with Q_o modified as above and the loaded Q is now defined from

$$\frac{1}{Q_L} = \frac{1}{Q_o} + \frac{1}{Q_1} + \frac{1}{Q_2}$$

$$\therefore \qquad Q_o = Q_L(1 + \gamma_1 + \gamma_2) \qquad (3.6)$$

Evaluating the power coupled into the cavity by loop 1 equation 3.4 becomes after modification

$$\frac{P}{P_o} = \frac{4\gamma_1(1 + \gamma_2)}{Q_o^2(\frac{\omega}{\omega_o} - \frac{\omega_o}{\omega})^2 + (1 + \gamma_1 + \gamma_2)}$$

To determine the power coupled to the load by the second loop it is necessary to know what fraction of the power coupled into the cavity is transmitted to the load. The contributions of the cavity and the load in dissipating the power coupled into the cavity are related by the reciprocals of their respective Q values. A fraction

$$\frac{1/Q_2}{1/Q_o + 1/Q_2} = \frac{\gamma_2}{1 + \gamma_2}$$

is coupled out of the cavity. The cavity insertion loss becomes

$$T(\omega) = \frac{P_T}{P_o} = \frac{4\,\gamma_1\,\gamma_2}{(1 + \gamma_1 + \gamma_2)^2 + Q_o^2(\frac{\omega}{\omega_o} - \frac{\omega_o}{\omega})^2} \qquad (3.7)$$

where P_T is transmitted power. The insertion loss is symmetrical in γ_1 and γ_2 and is therefore the same no matter what direction through the cavity power is coupled. The form of equation 3.7 is similar to one derived by means of an equivalent circuit using coupling transformers[12].

Measurements were made of voltage standing wave ratio and standing wave minima position on the input line as a function of frequency with the cavity loaded at terminal 2. The results are plotted in Figure 3.8. The connections to the cavity were reversed and power fed to terminal 2 with a load at terminal 1. Similar measurements were made and are plotted in

Figure 3.9. The coupling parameter information derived from these plots is summarized in Table 3.1

TABLE 3.1

Power Direction	Minimum V.S.W.R.	Type of Variation
1 → 2	2.56	Undercoupled
2 → 1	1.62	Overcoupled

This permits evaluation of γ_1 and γ_2

$$\frac{\gamma_1}{1+\gamma_2} = \frac{1}{2.56} \qquad \frac{\gamma_2}{1+\gamma_1} = 1.62$$

$$\therefore \quad \gamma_1 = 2.85 \qquad \gamma_2 = 6.25$$

The transmission loss of the cavity at resonance was measured as being between 1.5 and 1.6 db., fluctuations in indication occurring because of disturbances due to noise at the low signal levels employed. The experimental values of γ_1 and γ_2 when inserted into equation 3.7 indicate a transmission loss of 1.55 db. at resonance. The measurement of transmission loss confirms the values of the coupling parameters determined from standing wave measurements.

From Figure 3.8 and Figure 3.9 and using equations 3.2 and 3.3, a loaded Q value can be determined. The half-power bandwidth as indicated by both curves is 29.4 mc.

$$Q_L = 3000/29.4 = 102$$

$$Q_o = 102(1 + 2.85 + 6.25)$$

$$= 1030$$

To evaluate the magnitude of the velocity modulation imposed on the electron beam it is necessary to know the gap voltage causing it. The voltage across the gap can be defined

$$V = \int_{gap} E \cdot ds$$

To relate this to the power supplied to the cavity, a shunt resistance R_s is defined

$$R_s = \frac{(\int E \cdot ds)^2}{2P_c}$$

where P_c is the power dissipated within the cavity and R_s is defined along the path of integration, which is the cavity axis as travelled by the electron beam.

The value of R_s can be experimentally determined by first determining Q_o as above and then finding R_s/Q_o by perturbation of the cavity resonant frequency with the introduction of a dielectric material across the gap.

For a gap of length l and area A and a dielectric material of relative dielectric constant K, Sproul and Linder[13] have given the ratio R_s/Q_o in terms of the change in resonant wavelength $\Delta\lambda_c$.

$$\frac{R_s}{Q_o} = \frac{120\,l}{(K-1)A}\,\Delta\lambda_c$$

The result is derived by considering the cavity to be equivalent to a parallel LCR resonant circuit. In such a circuit the Q is defined by

$$Q_o = 2\pi f_c C R_s$$

where f_c is the resonant frequency

C is the capacity

R_s is the resistance shunted across the parallel LC combination

The additional capacity due to the introduction of a dielectric material of length l and area A with a relative dielectric constant of K is

$$C = \frac{(K-1)\,\epsilon_o\,A}{l}$$

In such a circuit

$$f_c = \frac{1}{2\pi\sqrt{LC}}$$

and for a small change in capacity ΔC

$$\Delta f_c = - \frac{f_c}{2C} \Delta C = \frac{-2\pi f_c (K-1) \epsilon_o A}{2 C l}$$

By eliminating the unknown quantity C from the relations for Δf_c and Q_o and converting to changes in resonant wavelength the above value for R_s/Q_o is determined.

A small polystyrene plug 4.36 mm in diameter was inserted across the gap and the resonant wavelength of the cavity was shifted 2.80 mm. With a gap of 4.5 mm and K = 2.55 at 3000 mc. the value Q_o = 1030 gives for the shunt resistance

$$R_s = 6.75 \times 10^4 \text{ ohms}$$

It is possible to determine the cavity gap voltage by relating the peak cavity power to the average power measured by the bolometer in the output line. The pulse repetition frequency was measured with a Type 514D Tektronix Oscilloscope and found to be 1072 p.p.s. With the 1.0 μsec. pulse length used this gives a duty cycle of 1/933.

The PRD 8.1 db fixed attenuator in the cavity output line as shown in Figure 3.5 reduces the power to the bolometer to 0.155 of that transmitted by the cavity. The value of γ_2 indicates 6.25 times as much power is transmitted to the load as is dissipated in the cavity. Therefore for an indicated bolometer power of P_B, the peak cavity power is

$$P_c = \frac{933 \ P_B}{6.25 \times 0.155} = \frac{V^2}{2R_s}$$

The computed value of $R_s = 6.75 \times 10^4$ ohms gives

$$V = 361\sqrt{P_B}$$

where V is the peak gap voltage

P_B is power measured in milliwatts delivered to the bolometer

3. The Deflection System Design

The Lecher wire pairs were built from standard 0.125" stock and for maximum resonant Q of a half wave section, the centre to centre spacing is 0.230". At the operating wavelength this determines the calculated value of V_m to be 1,515 volts.

The electron beam accelerating potential was chosen to be 10,000 volts. To be able to observe bunching displayed on the screen over the maximum angular range, without the velocity sensitivity reducing to zero somewhere throughout the bunch, the velocity sensitivity parameter was set equal to zero at points on the screen separated by 180°. This could be satisfied only by $\delta_{\pi/2}$. From equation 2.5b

$$\sqrt{V_m} + \frac{1}{4}\sqrt{V_s} = \sqrt{V_o}$$

At the operating wavelength of 10.00 cm. with V_m = 1,515 volts and V_o = 10,000 volts, the required value of V_s was:-

$$V_s = 59{,}740 \text{ volts}$$

The value of V_s is established by the spacing s between the two sets of Lecher wires.

$$V_s = 1.008 \times 10^7 \frac{s^2}{\lambda^2} \text{ volts}$$

and this completed the analyser design by fixing the centre to centre spacing as

$$s = 0.303"$$

On the basis of copper conductors the input impedance of a short circuited half wave transmission line adjusted for maximum Q and operating at 10 cm was computed to be[14]

$$Z = 8.5 \times 10^{-2} \text{ ohms}$$

To drive the Lecher wires from coaxial cable, a balanced to unbalanced line transformer or "balun" is required. Provision for matching the impedance

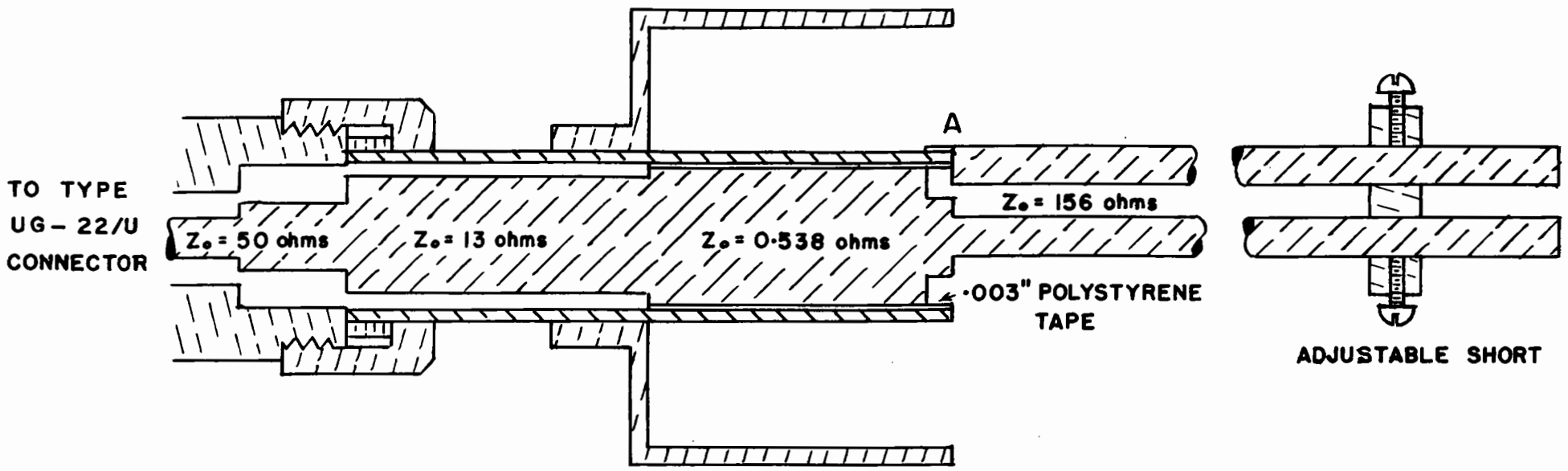

FIG. 3.10 LECHER WIRE PAIR, BALUN, AND IMPEDANCE MATCHING TRANSFORMER

at the input to the balun to the 50 ohm cable is also necessary. The details of the transformer and the matching section are shown in Figure 3.10.

The balanced pair of conductors forming the Lecher wire pair are tied directly to the inner and outer conductors of the coaxial line. A skirt has been placed around the coaxial line and extends one-quarter wavelength from the junction with the balanced line. The outer conductor of the coaxial line and the skirt form a second coaxial line. As the second coaxial line is in the form of a short circuited quarter wave section, the impedance between ground and the junction of the outer conductor of the main coaxial line with one of the wires forming the balanced pair (point A in Figure 3.10) is very high. With no loss of current to ground at point A, both conductors of the Lecher wire pair carry equal currents and if the distributed capacitance and conductance to ground is the same for each wire of the pair, the line is balanced.

The input impedance, Z_1, of a quarter wave section of line of characteristic impedance Z_o when terminated by a load impedance of Z_2 is given by

$$Z_1 = Z_o^2/Z_2$$

The characteristic impedance of the balun is 0.538 ohms, the dielectric being .003" polystyrene film. The above relation indicates that the Lecher wire impedance of 8.5×10^{-2} ohms is transformed to 3.4 ohms at the input to the balun. A quarter wave impedance matching transformer with a characteristic impedance of 13 ohms provides the transformation to 50 ohms to match the input connector and cable.

4. Operation and Adjustment

With the electron gun operating and a spot focused on the screen, excitation of the Lecher wires forming the analyser resulted in a pattern

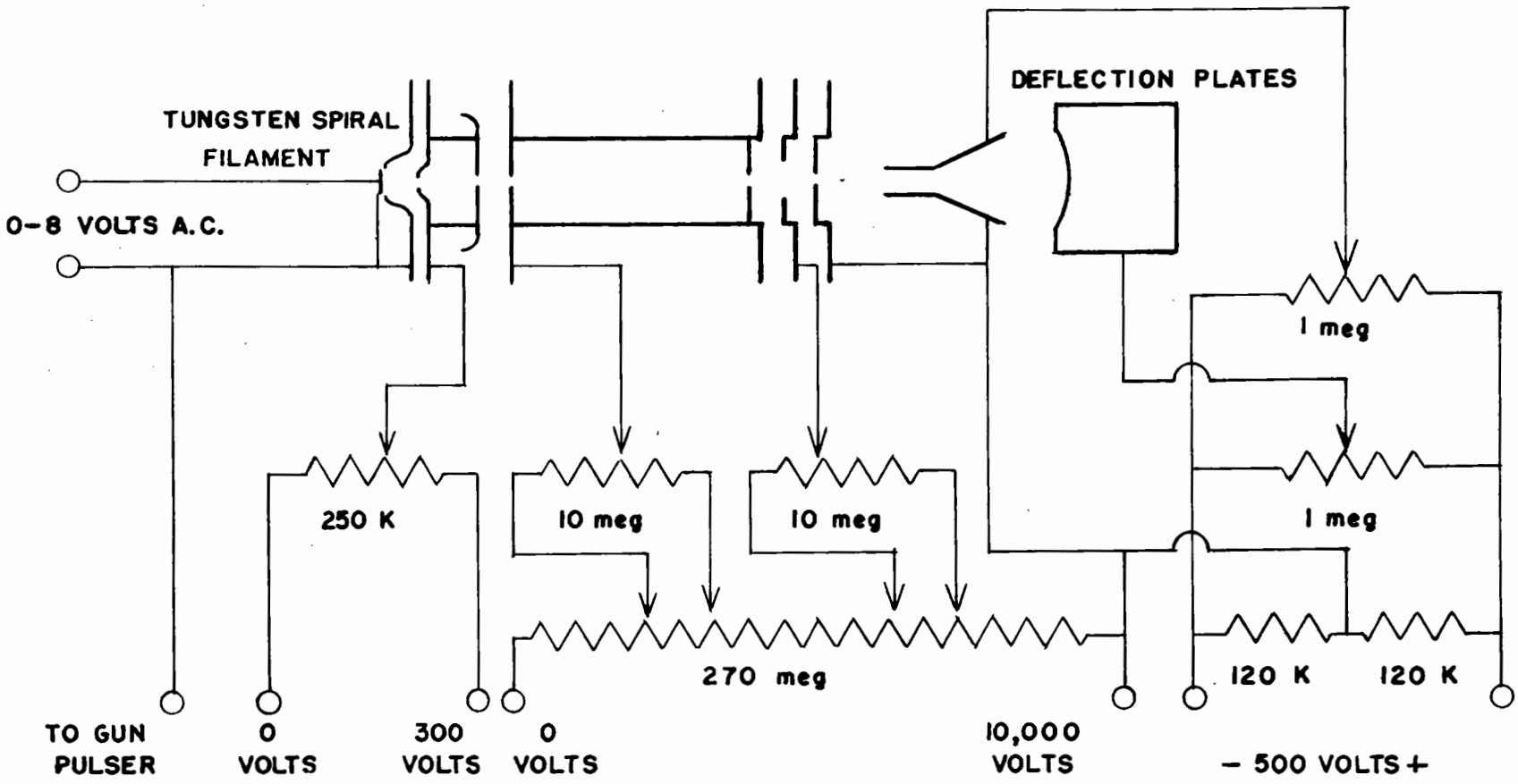

FIG. 3·11 ELECTRON GUN

of the form shown in Figure 3.12. Adjustment of the double stub tuners and the line stretchers permitted the proper phasing to obtain a circular trace. Patterns could be obtained without the use of the double stub tuners, indicating the input impedance to the Lecher wires and matching section was close to the required value, but the added facility of amplitude and phase adjustment prompted their use. The existence of a central spot due to undeflected electrons resulted from the fact that the decay time for the electron gun pulse was somewhat longer than that for the magnetron pulse. The bunching process was displayed on the circular trace as power was coupled to the cavity by means of the adjustable attenuator.

When first placed in operation, the electron gun produced on the fluorescent screen a focused image of the cathode which was too large for the purpose required. A 0.8 mm aperture was placed to sample the beam before it entered the analyser. It was found however, that no spot could be obtained on the screen for any setting of the electron gun deflection plate voltages. A small spot of light from the glowing tungsten filament was visible indicating that no obstruction to a straight electron path existed. It was concluded that the electron beam was being deviated from a straight path by the earth's magnetic field. Calculation indicated that the beam could depart from the axis by as much as 4 mm in a drift distance of 20 cm. For the large beam with no aperture the deflection system of the electron gun permitted some compensation of this departure and the beam was visible on the screen. The situation became more serious when the beam path was more accurately defined by the cavity central hole, the 0.8 mm aperture and the 2.5 mm square formed by the crossed Lecher wires. Some means had to be provided for removing the effect of the earth's field between the cavity and the analyser. This was accomplished by placing near the region a

fixed magnet whose position was adjusted for maximum beam transmission. The patterns indicate that beyond the analyser the earth's magnetic field causes further deviation. The central spot of the electron beam did not coincide with the spot of light from the filament.

5. Observations and Calculations

A series of photographs were taken illustrating the change in beam characteristics with increases in cavity gap voltage. Figure 3.13 indicates the bunching process just commencing; the bunching parameter being less than unity. In Figure 3.14 the bunching parameter exceeds unity and throughout the bunch electrons of three different velocities exist, but are not completely resolved. Figures 3.15, 3.16 and 3.17 show the depletion of electrons from regions outside the bunch and the bunch spreading out in phase as the modulation voltage increases.

Between the two infinite current peaks that result for bunching parameters greater than unity, electrons of three different velocities exist at one point in phase. The velocity sensitivity of the deflection system therefore makes it possible to determine the position of these infinite current peaks. At points inside the peaks the trace is not only more intense because of increased electron density but shows radial variations due to the triple valued character of the beam velocity. Outside the current peaks the trace is less intense and the width of the trace shows that the velocity is single valued.

Measurements of the phase angle between the current peaks permits calculation of the bunching parameter from equation 1.3. The results are summarized in Table 3.2 and are compared with the calculated values.

FIG. 3.12

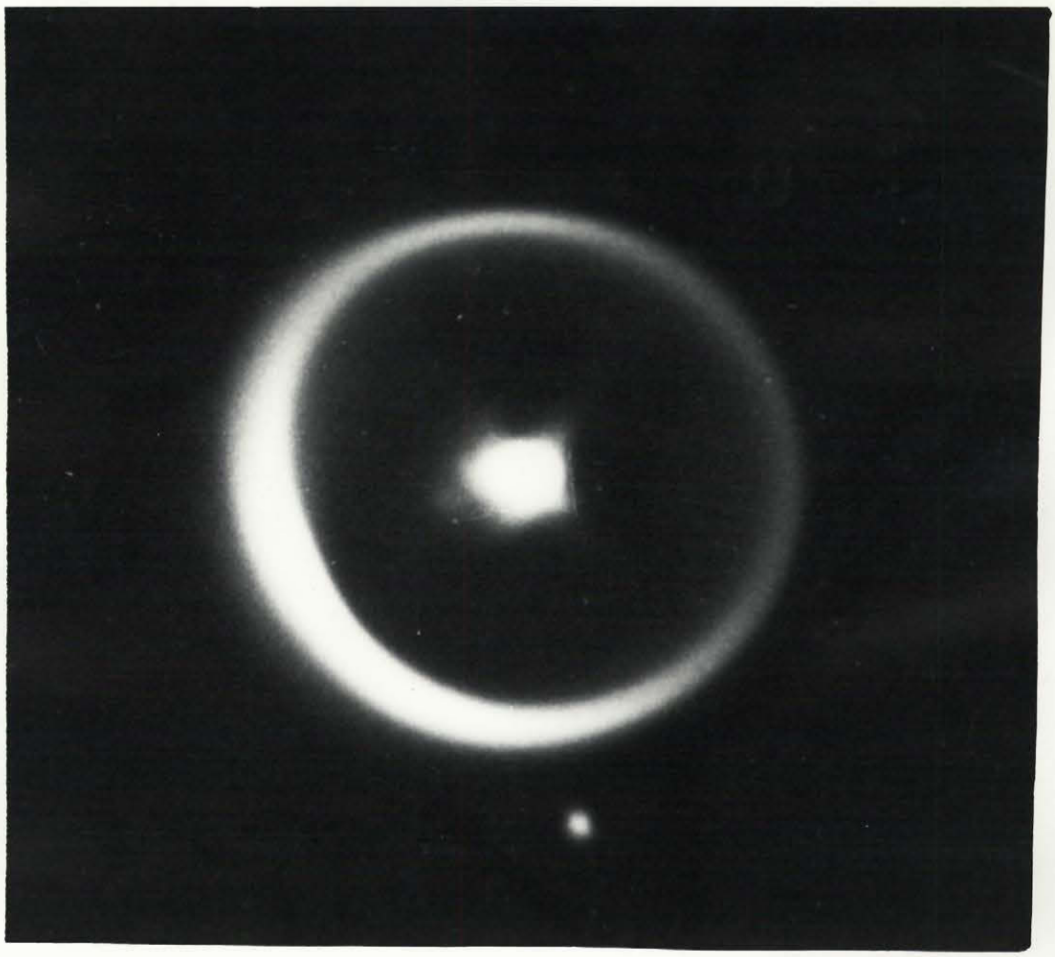

FIG. 3.13

OBSERVED BUNCHING PARAMETER 0.72

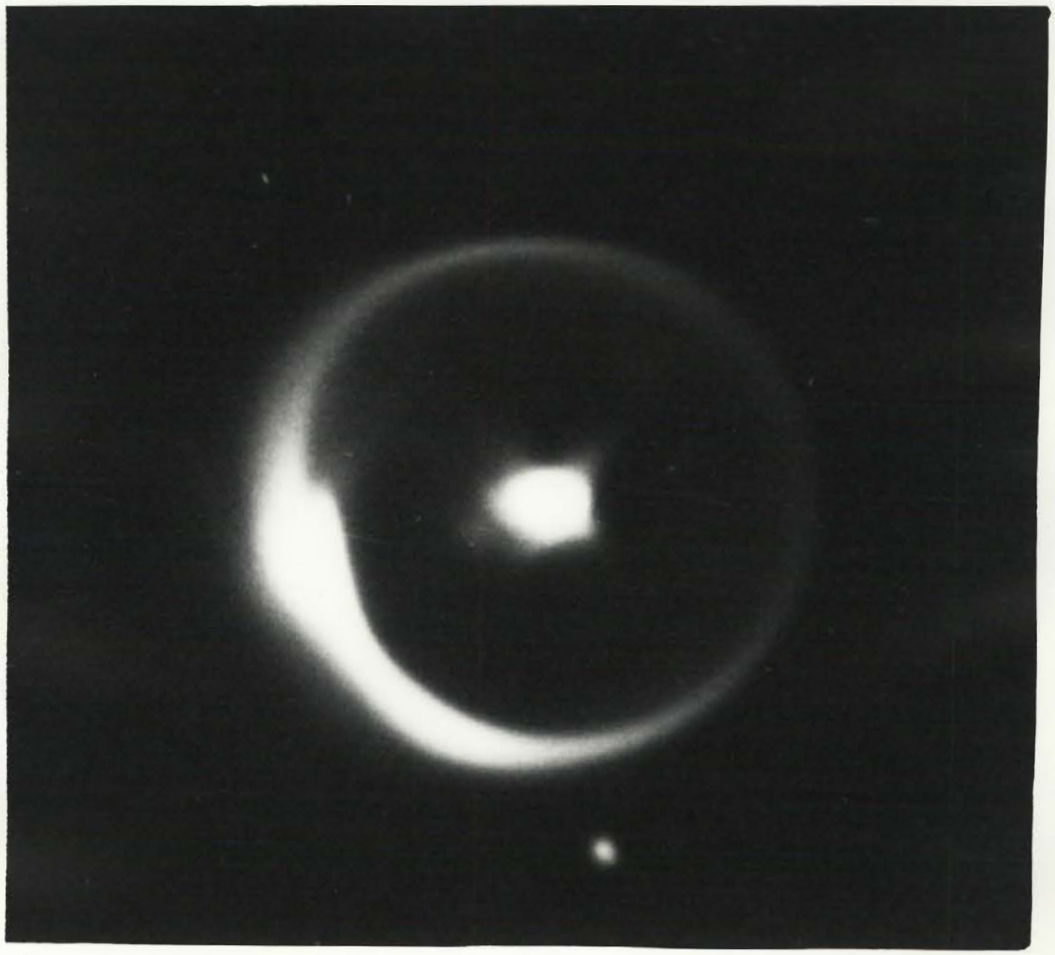

FIG. 3.14

OBSERVED BUNCHING PARAMETER 1.48

FIG. 3.15

OBSERVED BUNCHING PARAMETER 2.27

FIG. 3.16

OBSERVED BUNCHING PARAMETER 2.83

FIG. 3.17

OBSERVED BUNCHING PARAMETER 3.41

TABLE 3.2

Bolometer Power mw.	Calculated Bunching Parameter	Observed Bunch Angle	Observed Bunching Parameter
0.26	0.525	-	0.72 (estimated)
0.73	0.88	29.5°	1.48
2.60	1.66	106.0°	2.27
4.10	2.08	165.5°	2.83
6.00	2.52	228.0°	3.41

The calculated bunching parameter was based on the measured values of the following

Beam Voltage V_o = 10,300 volts

Drift Length l = 20.5 cm

Cavity Gap d = 0.45 cm

Frequency f = 3000 mc.

The observed value of the bunching parameter is greater than that calculated from power measurements. The beam patterns do exhibit the expected variations with increasing modulation. The observed and calculated values of the bunching parameter are compared in Figure 3.18. That they have a nearly constant ratio suggests that the discrepancy is due to inaccuracies in power measurement. The operation of a bolometer under pulsed conditions results in a power level indication somewhat lower than the average power being applied[15]. To account for the observed bunching parameter the power error or loss would need to be 2.6 db which seems somewhat excessive. Small but cumulative losses in cables and connectors associated with the measurement of power transmitted by the cavity could contribute to the discrepancy. Such losses at cable connectors were more apparent for connectors operating at higher power levels. Some showed a definite increase in temperature after a short period of operation. Similar losses occurring at the cavity connectors would not have produced a noticeable temperature increase because of the low average power involved. A possible error in the

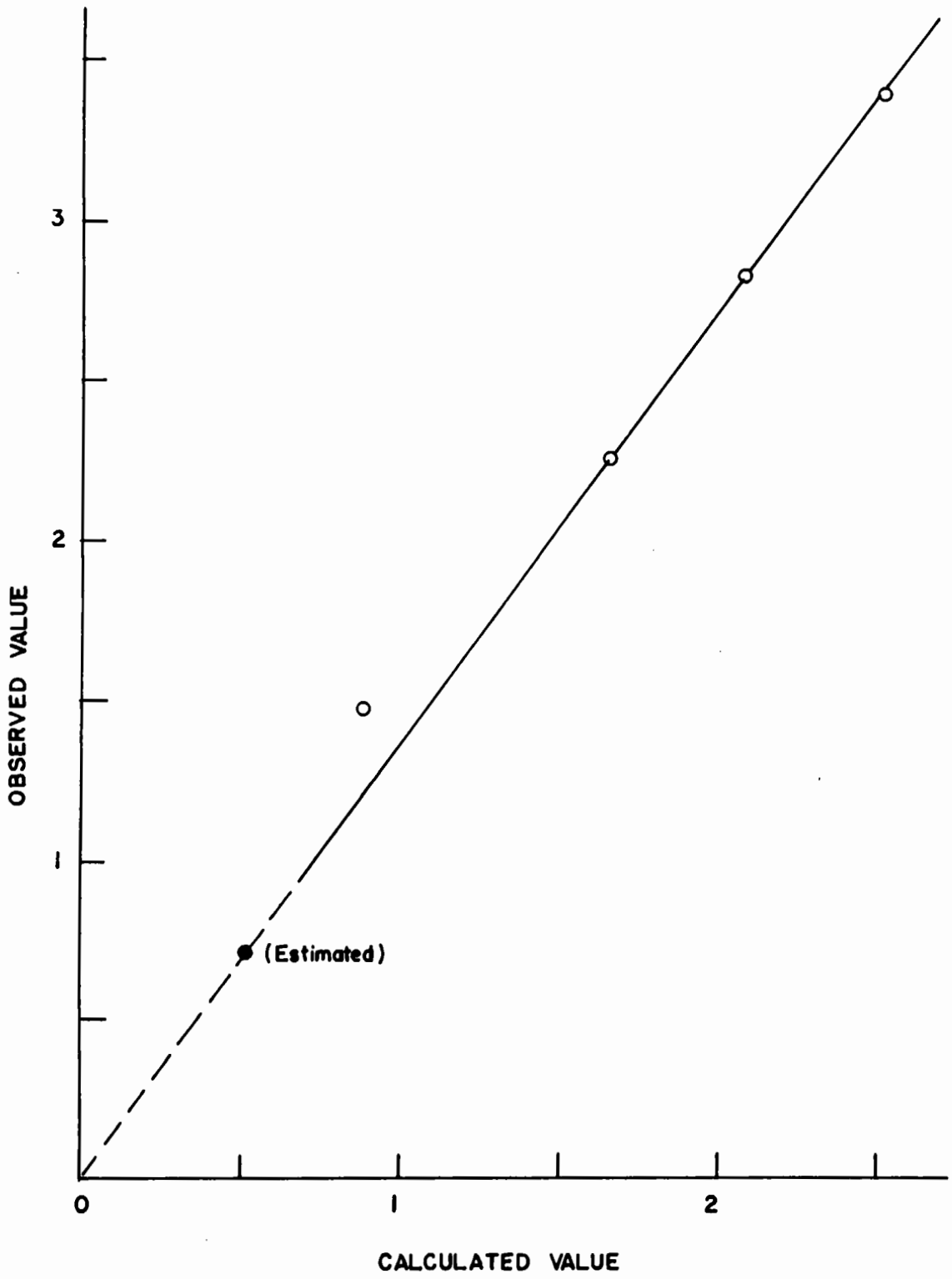

FIG. 3·18 COMPARISON OF OBSERVED AND CALCULATED BUNCHING PARAMETER

cavity shunt resistance determination could also account for the discrepancy.

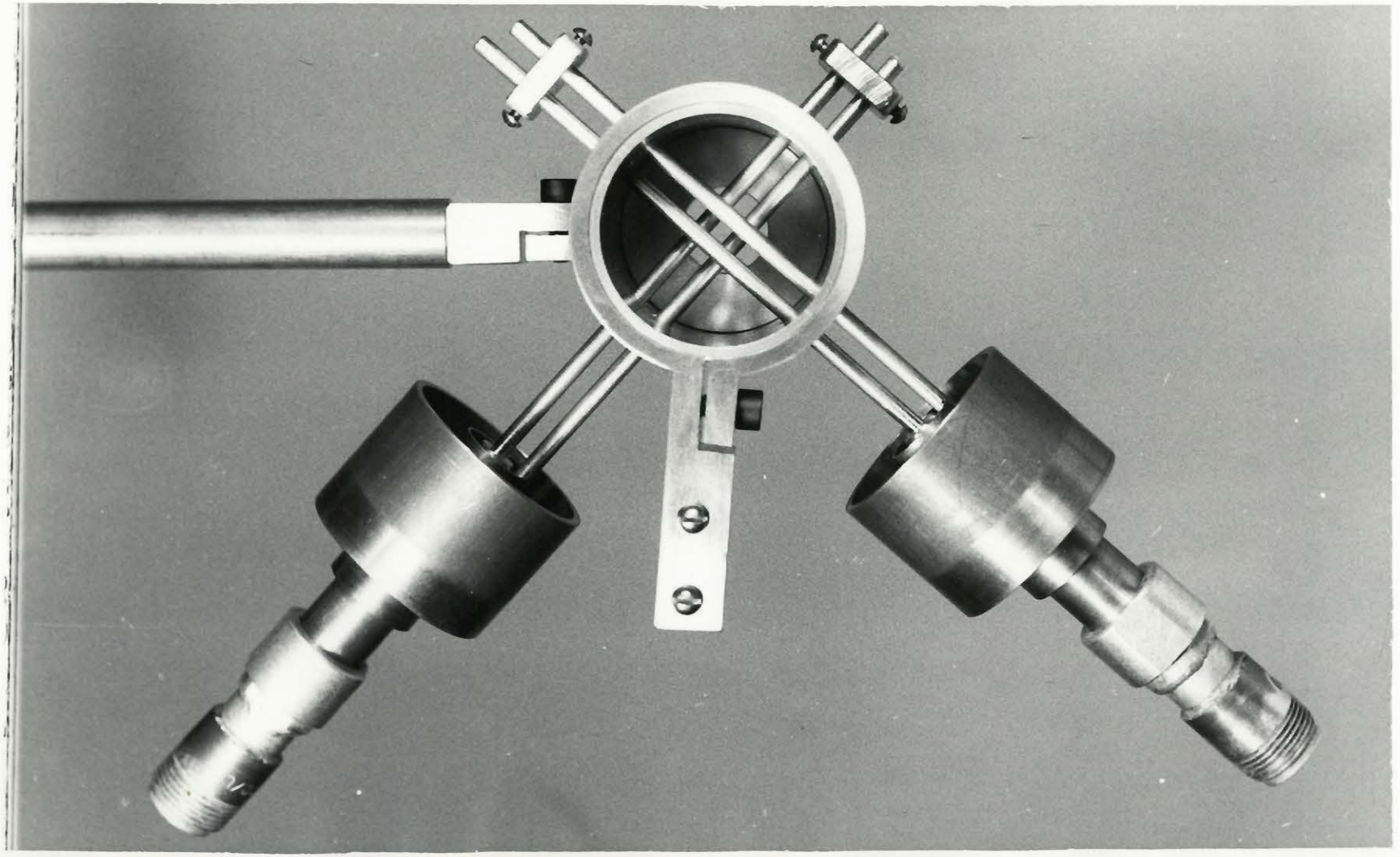

FIG. 3.19 DEFLECTION SYSTEM BEFORE ASSEMBLY

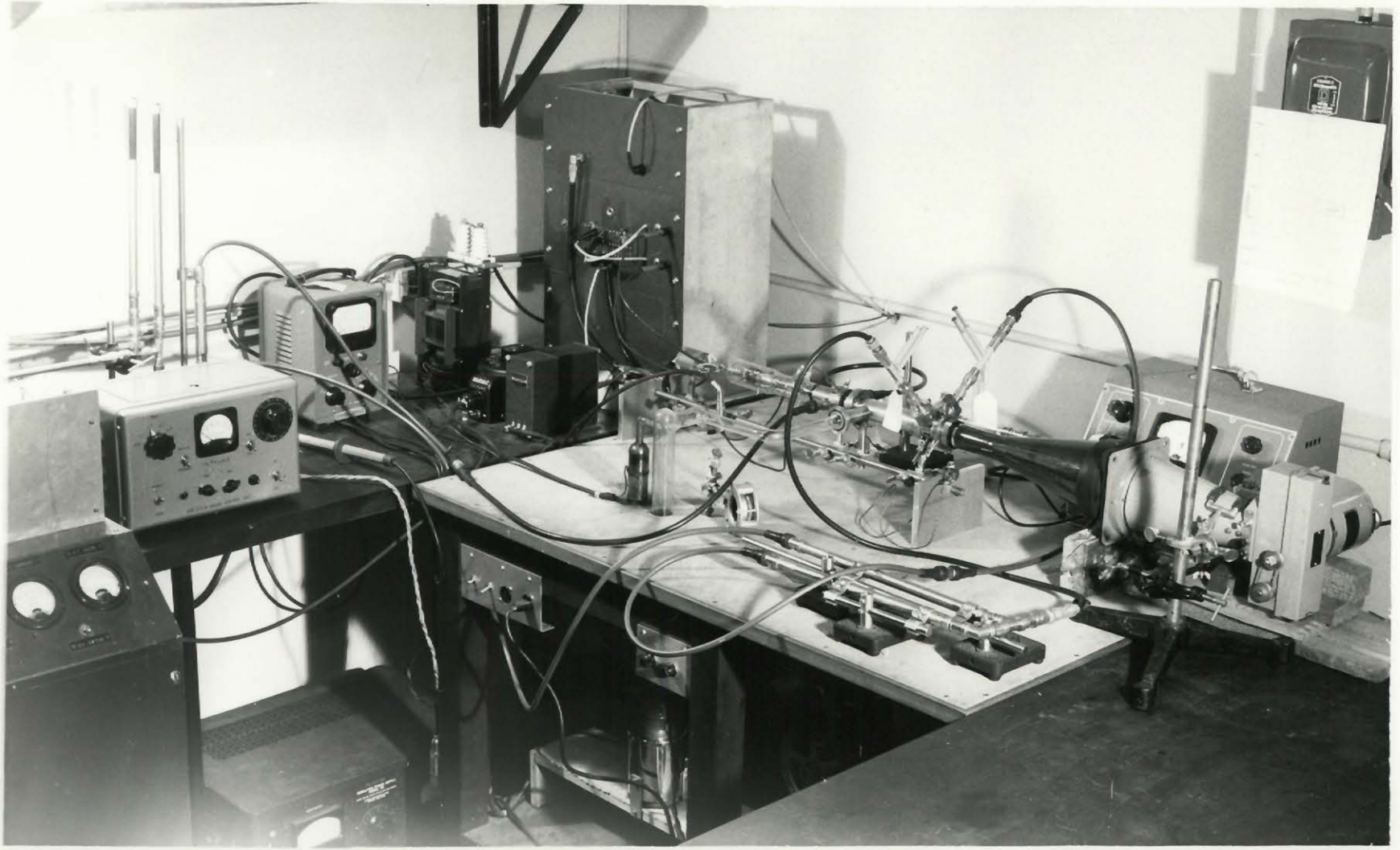

FIG. 3.20 THE EXPERIMENTAL SETUP

IV CONCLUSION

An analyser for the examination of velocity modulated electron beams has been designed and built. The type of analyser is applicable to the study of the electron bunching process employed in the operation of high frequency tubes. The analysis is achieved by displaying on a fluorescent screen the density and velocity variations in the electron beam at a particular point along the beam. The bunches of electrons are produced at the operating frequency and by driving the analyser from the same signal source as is used to modulate the electron beam, the scanning on the fluorescent screen is kept in exact synchronism with bunch production. This establishes a stationary trace which can be photographed and measured.

The analyser was operated at 10 cm using a magnetron as a source of radio frequency energy. The necessary electronic circuits were built to trigger the magnetron modulator and pulse the electron beam. Measurements were made of the parameters of the resonant cavity used to modulate the beam in order to permit calculation of the cavity gap voltage. A number of photographs of the beam trace were taken to illustrate the bunching process.

The principal difficulties encountered in the operation of the system were those associated with the electron beam. The diameter of the beam from the electron gun was too large for the display of satisfactory traces and necessitated the introduction of a limiting aperture. Of more serious import was the effect of the earth's magnetic field on the path of the electron beam. Calculation reveals that with beam voltages as high as 10,000 volts, the deviation from an axial path in a drift distance of the length employed can still be intolerably large. Shorter beam lengths and smaller cathodes to reduce beam size are recommended.

A circular trace was established on the fluorescent screen with no difficulty. With the application of a modulating signal the bunching process was apparent as one region of the trace increased in brilliance at the expense of other regions. The velocity sensitivity of the system is best illustrated in Figure 3.14 but spot size tends to obscure it. As the magnitude of the modulation voltage is increased the region of phase occupied by the bunch has the expected variation. The observed value of the bunching parameter is somewhat greater than that calculated from power measurements. That they have a nearly constant ratio suggests that the discrepancy is due to inaccuracies in power measurement. Some speculation on how these could arise has been made.

REFERENCES

1. A Type of Electrical Resonator - W.W. Hansen - Journal of Applied Physics 9, 654 (1938).
2. A High Frequency Oscillator and Amplifier, R.H. Varian and S.H. Varian- Journal of Applied Physics 10, 321, (1939).
3. Cathode Ray Bunching - D.L. Webster- Journal of Applied Physics 10, 501, (1939).
4. Microwave Electronics - J.C. Slater D. Van Nostrand Co. New York 1950, p. 226
5. Electron Repulsion Effects in a Klystron - L.A. Ware Proc. I.R.E. 33, 591 (1945)
6. Klystrons and Microwave Triodes - D.R. Hamilton, J.K. Knipp, J.B.H. Kuper, McGraw-Hill Inc. New York 1948, p. 217
7. Beam Analyser - N6-ORl-71 Task XIX NR 073 162 Technical Report No.5-3, L.R. Bloom, H.M. Von Foerster, University of Illinois, January 1953
8. Fields and Waves in Modern Radio - S. Ramo and J.R. Whinnery John Wiley and Sons Inc. New York 1949, p. 110
9. Integraltefel-Zweiter Teil - W. Grobner and N. Hofreiter Springer Verlag Wien 1950 p. 128 #67a
10. Microwave Transmission Design Data - Sperry Gyroscope Company Inc.
11. Microwave Electronics - J.C. Slater Reviews of Modern Physics 18(1946) p. 441
12. Technique of Microwave Measurements - C.G. Montgomery, M.I.T. Radiation Laboratory Series, McGraw-Hill Inc. New York 1947 p. 291
13. Resonant-Cavity Measurements - R.L. Sproul and E.G. Linder - Proc. I.R.E. 34, 305, (1946)

14. Radio Engineers Handbook - F.E. Terman -
McGraw-Hill Inc. New York 1943,p. 191

15. Handbook of Microwave Measurements - M. Wind and W. Rapoport
Polytechnic Institute of Brooklyn, p. 4-46